NASA -CR- 165,637

NASA Contractor Report 165637

NASA-CR-165637

1981 0002911

CRACK PROBLEMS FOR A RECTANGULAR PLATE
AND AN INFINITE STRIP

M. B. Civelek and F. Erdogan

LEHIGH UNIVERSITY
Bethlehem, Pennsylvania   18015

NASA

National Aeronautics and
Space Administration

Langley Research Center
Hampton, Virginia 23665

CRACK PROBLEMS FOR A RECTANGULAR PLATE

AND AN INFINITE STRIP*

by

M.B. Civelek and F. Erdogan
Lehigh University, Bethlehem, PA. 18015

Abstract

In this paper, the general plane problem for an infinite strip containing multiple cracks perpendicular to its boundaries is considered. The problem is reduced to a system of singular integral equations. Two specific problems of practical interest are then studied in detail. The first is the investigation of the interaction effect of multiple edge cracks in a plate or beam under tension or bending. The second problem is that of a rectangular plate containing an arbitrarily oriented crack in the plane of symmetry. Particular emphasis is placed on studying the problem of a plate containing an edge crack and subjected to concentrated forces. The plate has the dimensions of a standard compact tension specimen and is intended to simulate CTS.

1. Introduction

The plane problem for an infinite strip containing an edge crack simulating a single edge notch specimen, a beam, or a plate and the problem of a rectangular block with an edge or an internal crack simulating a compact tension specimen are two of the more widely studied geometries in fracture mechanics. Aside from the standard finite element methods (e.g. [1]), a wide variety of analytical and numerical methods have been used to solve the problem. Some of the significant techniques used in these studies are the Wiener-Hopf method (e.g. [2]), the method of weight functions (e.g. [3]), the method of Laurent series (e.g. [4,5]), the conformal mapping technique (e.g. [6]), the method of integral equations (e.g. [7,8]), and the method of boundary

-1-

N81-11419#

collocation (e.g. [9-11]). In this paper the basic problem of multiple cracks for an infinite strip is considered by using the method of singular integral equations. The paper has two objectives. The first is to provide the solution of the interaction problem for a beam or a plate containing two or three edge cracks perpendicular to the boundary and subjected to membrane loading or pure bending. The second is to give an analytical solution to the crack problem for a rectangular block or a compact tension specimen which is subjected to arbitrary crack surface tractions or concentrated (body) forces.

2. Integral Equations of the Problem.

The basic crack geometry under consideration is shown in Figure 1. It is assumed that $y=0$ is a plane of symmetry with respect to loading as well as crack geometry and the conditions of the plane strain or the generalized plane stress are satisfied. In addition to arbitrarily distributed crack surface tractions, the medium may be acted upon by arbitrarily located concentrated forces P shown in the figure. First, it may easily be shown that[*] for a pair of point dislocations with densities g and h located at the point (x_0, y_0) and defined by

$$\frac{\partial}{\partial x} [v(x, y_0+0) - v(x, y_0-0)] = g(x_0, y_0) \delta(x-x_0) ,$$

$$\frac{\partial}{\partial x} [u(x, y_0+0) - u(x, y_0-0)] = h(x_0, y_0) \delta(x-x_0) \qquad (1a,b)$$

the stress state in an infinite plane may be expressed as

$$\sigma_{xx}^d (x,y) = g(x_0, y_0) G_{xx}(x, y, x_0, y_0) + h(x_0, y_0) H_{xx}(x, y, x_0, y_0) ,$$

$$\sigma_{yy}^d (x,y) = g(x_0, y_0) G_{yy}(x, y, x_0, y_0) + h(x_0, y_0) H_{yy}(x, y, x_0, y_0) ,$$

$$\sigma_{xy}^d (x,y) = g(x_0, y_0) G_{xy}(x, y, x_0, y_0) + h(x_0, y_0) H_{xy}(x, y, x_0, y_0) , \qquad (2a-c)$$

where u and v are the x and y-components of the displacement and the influence functions are given by

[*]For example, by using complex potentials [12] or standard Fourier transforms.

-2-

$$G_{xx}(x,y,x_0,y_0) = \frac{2\mu}{\pi(1+\kappa)} \frac{(x_0-x)[(x_0-x)^2 - (y-y_0)^2]}{[(x_0-x)^2 + (y-y_0)^2]^2} \quad ,$$

$$H_{xx}(x,y,x_0,y_0) = \frac{2\mu}{\pi(1+\kappa)} \frac{(y-y_0)[(y-y_0)^2 + 3(x_0-x)^2]}{[(x_0-x)^2 + (y-y_0)^2]^2} \quad ,$$

$$G_{yy}(x,y,x_0,y_0) = \frac{2\mu}{\pi(1+\kappa)} \frac{(x_0-x)[3(y-y_0)^2 + (x_0-x)^2]}{[(x_0-x)^2 + (y-y_0)^2]^2} \quad ,$$

$$H_{yy}(x,y,x_0,y_0) = \frac{2\mu}{\pi(1+\kappa)} \frac{(y-y_0)[(y-y_0)^2 - (x_0-x)^2]}{[(x_0-x)^2 + (y-y_0)^2]^2} \quad ,$$

$$G_{xy}(x,y,x_0,y_0) = \frac{2\mu}{\pi(1+\kappa)} \frac{(y-y_0)[(y-y_0)^2 - (x_0-x)^2]}{[(x_0-x)^2 + (y-y_0)^2]^2} \quad ,$$

$$H_{xy}(x,y,x_0,y_0) = \frac{2\mu}{\pi(1+\kappa)} \frac{(x_0-x)[(x_0-x)^2 - (y-y_0)^2]}{[(x_0-x)^2 + (y-y_0)^2]^2} \quad . \qquad (3a\text{-}f)$$

In (3) μ is the shear modulus and $\kappa = 3-4\nu$ for plane strain and $\kappa = (3-\nu)/(1+\nu)$ for generalized plane stress, ν being the Poisson's ratio.

Similarly, for a pair of concentrated body forces P and -P (per unit thickness) acting in y direction at points (m,n) and (m,-n), respectively, the stresses in the plane may be expressed as follows:

$$\sigma_{xx}^p (x,y) = P\, Q_{xx}(x,y,m,n),$$

$$\sigma_{yy}^p (x,y) = P\, Q_{yy}(x,y,m,n),$$

$$\sigma_{xy}^p (x,y) = P\, Q_{xy}(x,y,m,n), \qquad (4a\text{-}c)$$

where

$$Q_{xx}(x,y,m,n) = \frac{1}{2\pi(1+\kappa)} \left\{ \frac{y-n}{(x-m)^2 + (y-n)^2} \left[\kappa-1 - \frac{4(x-m)^2}{(x-m)^2 + (y-n)^2}\right] \right.$$

$$\left. - \frac{y+n}{(x-m)^2 + (y+n)^2} \left[\kappa-1 - \frac{4(x-m)^2}{(x-m)^2 + (y+n)^2}\right] \right\} \quad ,$$

$$Q_{yy}(x,y,m,n) = \frac{1}{2\pi(1+\kappa)} \left\{ \frac{y-n}{(x-m)^2 + (y-n)^2} \left[-(\kappa+3) + \frac{4(x-m)^2}{(x-m)^2 + (y-n)^2} \right] \right.$$

$$\left. - \frac{y+n}{(x-m)^2 + (y+n)^2} \left[-(\kappa+3) + \frac{4(x-m)^2}{(x-m)^2 + (y+n)^2} \right] \right\} ,$$

$$Q_{xy}(x,y,m,n) = \frac{1}{2\pi(1+\kappa)} \left\{ \frac{x-m}{(x-m)^2 + (y-n)^2} \left[-(\kappa+3) + \frac{4(x-m)^2}{(x-m)^2 + (y-n)^2} \right] \right.$$

$$\left. - \frac{x-m}{(x-m)^2 + (y+n)^2} \left[-(\kappa+3) + \frac{4(x-m)^2}{(x-m)^2 + (y+n)^2} \right] \right\}. \quad (5a\text{-}c)$$

Let us now consider the stress state in an infinite strip $0 < x < H$ parallel to the y axis for which $y=0$ is a plane of symmetry. Using Fourier transforms and the conditions of symmetry it may be shown that

$$\sigma_{xx}^s(x,y) = -\frac{4\mu}{\pi} \int_0^\infty \left\{ \left[\alpha(A_1 + xA_2) + \frac{1+\kappa}{2} A_2 \right] e^{-\alpha x} \right.$$

$$\left. + \left[\alpha(A_3 + xA_4) - \frac{1+\kappa}{2} A_4 \right] e^{\alpha x} \right\} \cos\alpha y \, d\alpha,$$

$$\sigma_{yy}^s(x,y) = \frac{4\mu}{\pi} \int_0^\infty \left\{ \left[\alpha(A_1 + xA_2) + \frac{\kappa-3}{2} A_2 \right] e^{-\alpha x} \right.$$

$$\left. + \left[\alpha(A_3 + xA_4) - \frac{\kappa-3}{2} A_4 \right] e^{\alpha x} \right\} \cos\alpha y \, d\alpha,$$

$$\sigma_{xy}^s(x,y) = -\frac{4\mu}{\pi} \int_0^\infty \left\{ \left[\alpha(A_1 + xA_2) + \frac{\kappa-1}{2} A_2 \right] e^{-\alpha x} \right.$$

$$\left. - \left[\alpha(A_3 + xA_4) - \frac{\kappa-1}{2} A_4 \right] e^{\alpha x} \right\} \sin\alpha y \, d\alpha, \quad (6a\text{-}c)$$

where $A_1, \ldots, A_4$ are unknown functions of α and are determined from the boundary conditions at $x=0$ and $x=H$. It is clear that if one imposes the boundary conditions

$$\sigma_{xx}(0,y) = \sigma_{xy}(0,y) = \sigma_{xx}(H,y) = \sigma_{xy}(H,y) = 0, \quad -\infty < y < \infty , \quad (7)$$

on a solution for which the stress state is given by

$$\sigma_{ij}(x,y) = \sigma_{ij}^d(x,y) + \sigma_{ij}^p(x,y) + \sigma_{ij}^s(x,y), \quad (i,j) = (x,y), \quad (8)$$

-4-

where σ^d_{ij} is the sum of the stresses due to symmetric dislocations located at points (x_0, y_0) and $(x_0, -y_0)$ as given by (2) with $g(x_0, y_0) = g(x_0, -y_0)$ and $h(x_0, y_0) = -h(x_0, -y_0)$, one would obtain the formulation of a strip $0 < x < H$, $-\infty < y < \infty$ which is free of surface tractions, is subjected to concentrated forces P and -P, and contains the dislocations defined by (1) at (x_0, y_0) and $(x_0, -y_0)$. If the dislocations mentioned are the only defects in the strip, then by substituting from (2-6) and (8) into (7) and by inverting the Fourier transforms, one can determine the unknown functions $A_1, \ldots, A_4$ in terms of P, g, and h and thus, obtain the closed form solution of the problem. Needless to say, since the concentrated forces and the dislocations are "point functions", the solution for any number of symmetric forces and dislocations may. be obtained by a simple superposition of suitable solutions given by (2-8). Also note that the more general nonsymmetric solution may be obtained by expressing the strip solution (6) in terms of infinite Fourier transforms and by eliminating terms involving (y+n) in (5).

Instead of dislocations if the strip contains cracks along $c < x_0 = t < d$, $y_0 = B = $ constant under a given set of surface tractions, by integrating the solution found for the dislocations in t one would obtain a system of integral equations for the unknown density functions g and h which may now be considered as functions of t only. Referring now to Figure 1, let g(t), h(t), and g(t), -h(t) be the density functions defined by (1) for the cracks II and III, respectively for which $c < t < d$, $y_0 = \mp B$. Also, let the strip have an additional crack I along $a < x_0 = t < b$, $y_0 = 0$. Considering the symmetry of the problem, for crack I one may write

$$\frac{\partial}{\partial x} [u(x, +0) - u(x, -0)] = h(x) = 0 ,$$

$$\frac{\partial}{\partial x} v(x, +0) = -\frac{\partial}{\partial x} v(x, -0) = f(x), \quad a < x < b. \tag{9a,b}$$

In addition to concentrated forces $\mp P$ let the strip be subjected to the following crack surface tractions

-5-

$$\sigma_{yy}(x,0) = p_1(x), \quad \sigma_{xy}(x,0) = 0, \quad a<x<b \, , \qquad (10a,b)$$

$$\sigma_{yy}(x,B) = \sigma_{yy}(x,-B) = p_2(x) \, ,$$

$$\sigma_{xy}(x,B) = -\sigma_{xy}(x,-B) = p_3(x), \quad c<x<d \, . \qquad (11a,b)$$

Thus, the terms σ_{ij}^d in the superimposed stress state given by (8) must contain the contributions from crack I with the density functions $g=f$ and $h=0$, crack II with g and h, and crack III with g and $-h$.

Following the procedure obtained above, after some straightforward manipulations the functions $A_i(\alpha)$, $(i=1,\ldots,4)$ may be determined from the boundary conditions [7] as follows:

$$A_1(\alpha) = (2\alpha D)^{-1}\{[4\alpha^2 H^2-(\kappa-1)L_1]R_1 + [4\alpha^2 H^2-(\kappa+1)L_2]R_2$$

$$+ [(1-\kappa)L_3 + 2\alpha H(e^{-\alpha H}-\kappa e^{\alpha H})]R_3 + [(1+\kappa)L_3 - 2\alpha H(e^{-\alpha H}+\kappa e^{\alpha H})]R_4\},$$

$$A_2(\alpha) = D^{-1}[L_1 R_1+L_2 R_2+(2\alpha H e^{\alpha H}+L_3)R_3 + (2\alpha H e^{\alpha H}-L_3)R_4],$$

$$A_3(\alpha) = (2\alpha D)^{-1}\{[4\alpha^2 H^2+(\kappa-1)L_4]R_1 + [(\kappa+1)L_5-4\alpha^2 H^2]R_2$$

$$+[(\kappa-1)L_3+2\alpha H(\kappa e^{-\alpha H}-e^{\alpha H})]R_3 + [(1+\kappa)L_3-2\alpha H(\kappa e^{-\alpha H}+e^{\alpha H})]R_4\},$$

$$A_4(\alpha) = D^{-1}[L_4 R_1+L_5 R_2+(L_3+2\alpha H e^{-\alpha H})R_3 + (L_3-2\alpha H e^{\alpha H})R_4], \quad (12a\text{-}d)$$

where
$$D(\alpha) = e^{2\alpha H} + e^{-2\alpha H} - 4\alpha^2 H^2 - 2 \, , \qquad (13)$$

and the functions $L_i(\alpha)$ $(i=1,\ldots,5)$, and $R_i(\alpha)$, $(i=1,\ldots,4)$ are given in Appendix A. Thus, the complete solution of the problem is obtained once the density functions f, g, and h are determined. One may note that because of the assumed symmetry in formulating the problem the condition (10b) is automatically satisfied. Substituting then from (8) giving the combined stresses in the strip into the crack surface boundary conditions (10a), (11a) and (11b) one would obtain the system of integral equations to determine the functions f, g, and h as follows:

-6-

$$\frac{2}{\pi} \int_a^b \left[\frac{1}{t-x} + k_{11}(x,t) \right] f(t)dt + \frac{1}{\pi} \int_c^d k_{12}(x,t)g(t)dt$$

$$\frac{1}{\pi} \int_c^d k_{13}(x,t)h(t)dt = \frac{1+\kappa}{2\mu} \left[P\, k_{14}(x) + p_1(x) \right], \quad a < x < b ,$$

$$\frac{2}{\pi} \int_a^b k_{21}(x,t)f(t)dt + \frac{1}{\pi} \int_c^d \left[\frac{1}{t-x} + k_{22}(x,t) \right] g(t)dt$$

$$+ \frac{1}{\pi} \int_c^d k_{23}(x,t)h(t)dt = \frac{1+\kappa}{2\mu} \left[P\, k_{24}(x) + p_2(x) \right], \quad c < x < d,$$

$$\frac{2}{\pi} \int_a^b k_{31}(x,t)f(t)dt + \frac{1}{\pi} \int_c^d k_{32}(x,t)\, g(t)dt$$

$$+ \frac{1}{\pi} \int_a^b \left[\frac{1}{t-x} + k_{33}(x,t) \right] h(t)dt = \frac{1+\kappa}{2\mu} \left[Pk_{34}(x) + p_3(x) \right], \quad c < x < d,$$

$$\tag{14a-c}$$

where the kernels $k_{ij}(x,t)$ and the functions k_{i4}, $(i,j=1,2,3)$ are given in Appendix B.

If the cracks are internal cracks as shown in Figure 1, then the solution of the integral equations (14) must satisfy the following single-valuedness conditions:

$$\int_a^b f(t)dt = 0,$$

$$\int_c^d g(t)dt = 0,$$

$$\int_c^d h(t)dt = 0 . \tag{15a-c}$$

For the internal cracks the integral equations (14) have ordinary Cauchy kernels and their solution may be obtained in a simple manner by using, for example, the technique described in [13]. After determining the density functions f, g, and h, the stress intensity factors at the crack tips may be defined and evaluated as follows:

$$k_1(a) = \lim_{x \to a} \sqrt{2(a-x)}\, \sigma_{yy}(x,0) = \frac{4\mu}{1+\kappa} \lim_{x \to a} \sqrt{2(x-a)}\, f(x),$$

$$k_1(b) = \lim_{x \to b} \sqrt{2(x-b)}\, \sigma_{yy}(x,0) = - \frac{4\mu}{1+\kappa} \lim_{x \to b} \sqrt{2(b-x)}\, f(x) ,$$

$$k_1(c) = \lim_{x \to c} \sqrt{2(c-x)} \; \sigma_{yy}(x,B) = \frac{2\mu}{1+\kappa} \lim_{x \to c} \sqrt{2(x-c)} \; g(x),$$

$$k_2(c) = \lim_{x \to c} \sqrt{2(c-x)} \; \sigma_{xy}(x,B) = \frac{2\mu}{1+\kappa} \lim_{x \to c} \sqrt{2(x-c)} \; h(x),$$

$$k_1(d) = \lim_{x \to d} \sqrt{2(x-d)} \; \sigma_{yy}(x,B) = - \frac{2\mu}{1+\kappa} \lim_{x \to d} \sqrt{2(d-x)} \; g(x) ,$$

$$k_2(d) = \lim_{x \to d} \sqrt{2(x-d)} \; \sigma_{xy}(x,B) = - \frac{2\mu}{1+\kappa} \lim_{x \to d} \sqrt{2(d-x)} \; h(x), \qquad \text{(16a-f)}$$

where k_1 and k_2 are Modes I and II stress intensity factors.

For edge cracks, the asymptotic behavior of the kernels and the nature of the singularity of the solution of the integral equations were treated in [14]. In the problem under consideration the asymptotic analysis of the kernels have been performed for the limiting cases of (a=0, b<H), (a>0, b=H), (c=0, d<H), (c>0, d=H), and (c=0, d=H). Omitting the analytical details, only the results are given in equations (14) and Appendix B. From (14) and Appendix B it may be seen that the singular part of the kernels on the main diagonal of the system of integral equations, for example, for a=0 and c=0 is given by

$$k_s(x,t) = \frac{1}{t-x} - \frac{1}{t+x} + \frac{6x}{(t+x)^2} - \frac{4x^2}{(t+x)^3} . \qquad (17)$$

The kernel $k_s(x,t)$ is a generalized Cauchy kernel. The peculiarity of this particular generalized Cauchy kernel is that even though $k_s(0,t)=0$ for $0<t\leq H$ and $k_s(x,0) = 0$ for $0<x\leq H$, the part of k_s excluding the Cauchy kernel, i.e., the sum of the last three terms in (17), becomes unbounded as x and t approach the end point zero simultaneously, that is, for $t \to 0$ with x=At, A being an arbitrary nonzero constant. Because of this property it was shown in [14] that for a=0 f(a) and for c=0 g(c) and h(c) would be bounded. This is also the result one would expect on physical grounds. The technique for solving the edge crack has also been described in [14].

3. The Results and Discussion
    (a) The Infinite Strip.

The first problem considered is the problem of interaction of two symmetric internal cracks in an infinite strip under uniform tension. Referring to Figure 1 and to the integral equations (14), for this

crack geometry we have a=b, c=H-d, P=0, $p_2(x) = -\sigma_0$, and $p_3(x) = 0$. Some calculated results are given in Table 1. The stress intensity factors obtained for $\ell/H = 0.05$, $\ell=(d-c)/2$ are indistinguishable from the values given in [15] which are obtained for an infinite plane. Note that as the crack distance 2B decreases k_1 also decreases and k_2 becomes more significant. The angle θ shown in the table is a measure of the probable crack growth direction in brittle materials and is obtained from the simple assumption that along this direction $\sigma_{\theta\theta}(r,\theta)$ is maximum, where $r << H-d$ [16]. Here $\theta>0$ means that the cracks would propagate away from each other.

Some results for the problem of interaction of two symmetric edge cracks in a strip under uniform tension or pure bending away from the crack region are given in Figures 2-5. For this geometry we have a=b, c=0, and d<H. The figures also show the values of k_1 for a single edge crack (as the dashed line). For a single edge crack k_2 and θ are zero. Again note that k_1 is smaller than the corresponding single edge crack value, k_2 becomes more significant as B decreases, and in brittle materials the cracks would tend to propagate away from each other.

The results for three edge cracks in a strip under uniform tension or bending are shown in Figures 6-11. In all cases $k_2(d)<0$ meaning that the outside cracks would again grow away from the crack in the middle. It may be observed that for a strip under tension and pure bending the Mode I stress intensity factor for the middle crack is less than that of the outer cracks which, in turn, is less than the corresponding single crack value. Comparing the results given in Figures 2-5 with those given in Figures 6-9, it may be seen that the presence of the middle crack "relaxes" the stress state in the strip resulting in smaller stress intensity factors. Figure 10 shows the effect of the crack depth on the stress intensity factors. For b=d<<(B,H) the results reduce to the value for a single edge crack in a semi-infinite plane, i.e., $k_1 = 1.1216$, $k_2 = 0$. As crack lengths increase, first the interaction effect and then the free boundary effect (from x=H) dominate. Consequently the values of $k_1(b)$ and $k_1(d)$ somewhat decrease before increasing sharply. Figure 11 shows an example for a beam or plate

Table 1. Stress intensity factors in a strip containing
two symmetric internal cracks, $\ell=(d-c)/2$.

ℓ/H	B/ℓ	$k_1/\sigma_0\sqrt{\ell}$	$k_2/\sigma_0\sqrt{\ell}$	$\theta(°)$
	0.5	0.7797	-0.1175	16.430
	1.0	0.8512	-0.0616	8.194
	1.5	0.9052	-0.0308	3.887
0.05	2.0	0.9395	-0.0163	1.992
	5.0	0.9953	-0.0001	0.157
	10.0	1.0053	-0.00001	0.014
	20.0	1.0060	0.0000	0.000
	0.5	0.7992	-0.1199	16.363
	1.0	0.8749	-0.0624	8.076
	1.5	0.9310	-0.0307	3.774
0.1	2.0	0.9660	-0.0162	1.920
	5.0	1.0219	-0.0001	0.106
	10.0	1.0247	-0.00001	0.003
	20.0	1.0248	0.0000	0.000
	0.5	0.8846	-0.2570	15.578
	1.0	0.9749	-0.0656	7.634
	1.5	1.0437	-0.0330	3.648
0.2	2.0	1.0839	-0.0155	1.641
	5.0	1.1096	-0.0001	0.019
	10.0	1.1097	0.0000	0.000

under three point bending[(*)]. Here the stress intensity factor for the outer crack becomes zero for B=4H (the load distance), decreases as B approaches zero and hence goes through a maximum for a certain value of B/H which may depend on the crack depth.

(b) The Compact Tension Specimen.

The problems of the rectangular plate and the compact tension specimen are solved by letting c=0 and d=H in the basic strip problem (see Figure 1). In this case both ends of the outer cracks are treated as if they are the free ends of an edge crack. The integral equations (14) with the generalized Cauchy kernels are still valid. In all the problems considered for this geometry, it is assumed that the tractions p_2 and p_3 on the surfaces of the outer cracks are zero.

The calculated stress intensity factors for a square plate containing an internal crack and subjected to uniform tension perpendicular to the crack are shown in Table 2. Here the parameters e and λ represent the eccentricity in the crack location and the relative crack length, e=0 being the symmetrically located central crack. A limited comparison of the stress intensity factors calculated in this paper and that obtained in [5] for the crack geometry used in [5] is given in Table 3. In [5] only $k_1(b)$, the greater of the two stress intensity factors, is given. The agreement appears to be quite good.

The stress intensity factor in a square plate containing a symmetrically located central crack and subjected to concentrated wedge forces P (per unit thickness) in the middle of the crack is shown in Table 4. The table also shows the results given in [11]. Again, the agreement appears to be very good. Note that for the infinite plate the result is $k_1 = P/\pi\sqrt{\ell}$ where $\ell = (b-a)/2$. The effect of the location of the concentrated wedge force on the stress intensity factor is shown in Figure 12 for a specific crack geometry.

[(*)] In Figure 11 the strength of material solution is used for the uncracked strip. See [7] and [8] for the effect of concentrated forces and through thickness stress distribution obtained from the elasticity solution on the stress intensity factors.

Table 2. Stress intensity factors in a uniformly loaded square plate containing an internal crack. $c=0$, $d=H$, $B=H/2$, $e=(b+a-H)/H$ (eccentricity), $\lambda=(b-a)/H$, $p_1(x)=-\sigma_0$, $p_2=0$, $p_3=0$ (see Fig. 1 and eq. 11)

e	λ	$k_1(a)/\sigma_0\sqrt{(b-a)/2}$	$k_1(b)/\sigma_0\sqrt{(b-a)/2}$
	0.1	1.0140	1.0140
	0.2	1.0554	1.0554
	0.3	1.1233	1.1233
	0.4	1.2162	1.2162
0	0.5	1.3339	1.3339
	0.6	1.4810	1.4810
	0.7	1.6774	1.6774
	0.8	1.9914	1.9914
	0.9	2.7129	2.7129
	0.1	1.0139	1.0140
	0.2	1.0553	1.0559
	0.3	1.1234	1.1269
0.1	0.4	1.2172	1.2326
	0.5	1.3370	1.3919
	0.6	1.4880	1.6669
	0.7	1.6972	2.3186
	0.1	1.0151	1.0161
	0.2	1.0596	1.0692
0.2	0.3	1.1345	1.1759
	0.4	1.2469	1.3870
	0.5	1.4278	1.9113
	0.1	1.0246	1.0304
0.3	0.2	1.0975	1.1527
	0.3	1.2431	1.5170
0.4	0.1	1.0789	1.1227

Table 3. Comparison of the stress intensity factors calculated from (14) and that given in [5] for a rectangular plate under uniform tension. $p_1=-\sigma_0$, $a=0.545H$, $b=0.755H$, $\ell=(b-a)/2$.

B/H	0.25	0.50	0.71	1.0	∞
$k_1(a)/\sigma_0\sqrt{\ell}$ (Eq. 14)	1.2000	1.0617	1.0406	1.0382	
$k_1(b)/\sigma_0\sqrt{\ell}$ (Eq. 14)	1.2061	1.0655	1.0518	1.0507	1.0507
$k_1(b)/\sigma_0\sqrt{\ell}$ [5]	1.205	1.066	1.050	1.050	1.0507

Table 4. Stress intensity factor in a square plate containing a central crack which is loaded by wedge forces. $B=H/2$, $a=H-b$, $\ell=(b-a)/2$, $p_1(x)=-P\delta(x)$.

ℓ/H	$k_1/(P/\pi\sqrt{\ell})$ (Eq. 14)	$k_1/(P/\pi\sqrt{\ell})$ (Ref. [11])
0.05	1.02907	1.0279
0.10	1.11278	1.1115
0.15	1.2514	1.2499
0.20	1.4437	1.4418
0.25	1.6889	1.6866
0.30	1.9921	1.9894
0.35	2.3804	2.3772
0.40	2.9561	2.9523
0.45	4.1717	4.1665

The results for a rectangular plate containing an edge crack and subjected to uniform tension are given in Figure 13 and Tables 5 and 6 (see insert in Figure 13). The figure shows the effect of the crack length on the stress intensity factor for two values of B/H. The effect of length-to-width ratio B/H of the plate on the stress intensity factor is given in Table 5. For B/H = 2 the result is practically the same as that found for an infinite strip with an edge crack. Table 6 shows the effect of the crack length on the stress intensity factor in a square plate containing an edge crack and subjected to uniform tension (see insert in Figure 13). The table also shows the results given in [6]. It is seen that the agreement between the two sets of values is very good.

Table 5. Stress intensity factor in a uniformly stressed rectangular plate containing an edge crack. The crack length b=0.5H, a=0, $p_1(x) = -\sigma_0$.

B/H	0.25	0.5	1.0	2.0	∞
$k_1(b)/\sigma_0\sqrt{b}$	4.8298	3.0103	2.8263	2.8254	2.8250

Table 6. Stress intensity factor in a uniformly stressed square plate with an edge crack. a=0, B=0.5H, $p_1(x) = -\sigma_0$.

b/H	0.1	0.2	0.3	0.4	0.5	0.6	0.7	0.8
$k_1(b)/\sigma_0\sqrt{b}$ (Eq. 14)	1.2295	1.4877	1.8483	2.3245	3.0103	4.1525	6.4044	12.0013
$k_1(b)/\sigma_0\sqrt{b}$ (Ref.[6])	1.23	1.49	1.85	2.32	3.01	4.15	6.40	12.0

The results for a square plate with an edge crack and subjected to concentrated wedge forces P (per unit thickness) on the crack surfaces are given in Figure (14). Here the variable is the location of

the wedge force. As m→b the stress intensity factor would tend to the infinite plate value given by

$$k_1(b) = \frac{\sqrt{2}}{\pi\sqrt{b-m}} \frac{P}{} . \tag{18}$$

That is, it becomes unbounded. Also, as m→0 due to the "bending" effects the stress intensity factor would again increase. Hence, $k_1(b)$ goes through a minimum for a certain value of the load distance m. Similar results have been observed in [8] for an infinite strip with an edge crack which is subjected to a concentrated wedge force.

The remaining results in this paper concern an edge-cracked rectangular plate having the overall dimensions of a compact tension specimen which is under a pair of concentrated (body) forces P only. The geometry of the CTS is given by Figure 15. Referring also to Figure 1, it may be seen that W=0.8H, B=0.48H, m=0.2H, and n=0.32H. First, one may note that the effect of n, the load distance in y-direction on the stress intensity factor is rather insignificant. This may be seen from Table 7. As seen from Table 8, this is not the case for the load distance m in x-direction. It may be observed that for large values of m the stress intensity factor becomes negative. This is due to the fact that in the uncracked plate under concentrated loads ∓P the elasticity solution would give compressive stresses on part of the y=0 plane.

Table 7.   The effect of load distance n in y-direction on the stress intensity factor in a compact tension specimen under concentrated forces P. B=0.48H, m=0.2H, b=0.6H (see Figure 1).

n/H	0.32	0.3	0.2	0.1	0.05	0.01	0
$k_1(b)/(P\sqrt{b}/H)$	7.8487	7.8489	7.8492	7.8479	7.8480	7.8257	7.8549

Table 8. The effect of load distance m in x-direction on the stress intensity factor in a compact tension specimen under concentrated forces P. B=0.48H, n=0.32H, b=0.6H (Figure 1)

m/H	0	0.2	0.4	0.6	0.8	0.85	1.0
$k_1(b)/(P\sqrt{b}/H)$	10.2859	7.8492	5.3738	2.7207	0.4255	-0.02137	-1.4287

Table 9. Stress intensity factor for the compact tension specimen under concentrated forces P. m=0.2H, n=0.32H, B-0.48H, $k^*=k_1(b)/(P\sqrt{b}/H)$ (Figures 1 and 15).

b/H	0.50	0.52	0.54	0.56	0.58	0.60	0.62	0.64
k^*	6.1535	6.4122	6.7042	7.0341	7.4130	7.8487	8.3525	8.9385
b/H	0.66	0.68	0.70	0.72	0.74	0.76	0.78	0.80
k^*	9.6294	10.4387	11.3997	12.5507	13.9435	15.6493	17.7694	20.4519

The stress intensity factor for the compact tension specimen corresponding roughly to the standard load location m=0.2H, n=0.32H (Figures 1 and 15) is given in Table 9. The same results calculated in terms of the standard A/W values shown in Figure 15 and normalized with respect to $K_0=P/\sqrt{W}$ are given also in Table 10 (second column). For practical applications the stress intensity factors given in Table 10 may be approximated by, for example, a polynomial through a least square curve fit in the following form:

$$K = \frac{P}{\sqrt{W}} \left(\frac{A}{W} \right)^{\frac{1}{2}} \sum_{n=0}^{N} c_n (A/W)^n . \tag{19}$$

It should be noted that K which appears in (19) and in Table 10 is the standard Mode I stress intensity factor used in fracture mechanics and is related to the stress intensity factor $k_1(b)$ defined in (16) by

$$K = \sqrt{\pi} \, k_1(b) . \tag{20}$$

-16-

Table 10. Stress intensity factor for the compact tension specimen under concentrated forces P. $n=0.4W$, $m=0.25W$, $B=0.6W$, $H=1.25W$, $K_0=P/\sqrt{W}$ (Figures 1 and 15).

A/W	$K(b)/K_0$ (Eq. 14)	$K(b)/K_0$ (Eq. 19)	$K(b)/K_0$ (Ref. 10)
0.375	6.8981	6.9272	6.8177
0.400	7.3304	7.3182	7.2787
0.425	7.8102	7.7844	7.7829
0.450	8.3449	8.3264	8.3396
0.475	8.9501	8.9462	8.9603
0.500	9.6381	9.6499	9.6591
0.525	10.4263	10.4484	10.2989
0.550	11.3364	11.3598	11.3643
0.575	12.4020	12.4111	12.2337
0.600	13.6465	13.6427	13.6541
0.625	15.1204	15.1007	15.1132
0.650	16.8832	16.8594	16.8569
0.675	19.0155	19.0041	18.9659
0.700	21.6283	21.6442	21.5518
0.725	24.8794	24.9146	24.7719
0.750	29.0000	28.9787	28.8558

Table 11. Coefficients c_n which appear in Equation (19).

N	c_0	c_1	c_2	c_3	c_4	c_5	c_6	c_7
3	-43.252	336.265	-709.559	529.552				
4	171.451	-1261.74	3664.38	-4693.42	2298.41			
5	-207.428	2006.98	-7369.26	13530.5	-12437.1	4668.26		
6	27.606	-91.036	44.302	448.366	-630.114	-134.171	512.814	
7	23.663	-70.262	38.850	310.498	-406.739	-45.894	107.933	224.955

Table 11 gives the coefficients c_n of the polynomial (19) for various values of N. For N=6 the (approximate) results calculated from (19) are given in Table 10 (column 3) along with the values calculated from the expression given in [10] (column 4). These results show that for a compact tension specimen, particularly in analyzing fatigue crack propagation data, the expression given by (19) or that developed in [10] may be used with a certain degree of confidence.

References

1.   W.K. Wilson, "Finite Element Methods for Elastic Bodies Containing Cracks", Methods of Analysis and Solutions of Crack Problems, G.C. Sih, ed., p. 484-515, Noordhoff Int. Publ. Leyden, 1973.

2.   W.T. Koiter, "Rectangular Tensile Sheet with Symmetric Edge Cracks", J. Appl. Mech., Vol. 32, Trans. ASME, pp. 237-242, 1965.

3.   H.F. Bueckner, "Weight Functions for the Notched Bar", ZAMM, Vol. 51, pp. 97-109, 1971.

4.   M. Isida, "Method of Laurent Series Expansion for Internal Crack Problems", Method of Analysis and Solutions of Crack Problems, G.C. Sih, ed., pp. 56-130, Noordhoff Int. Publ. Leyden, 1973.

5.   H. Terada and M. Isida, "Analysis of Stress Intensity Factors for Eccentric Cracks in Plate and Strip", NAL TR-436, Dec. 1975, National Aerospace Lab., Tokyo, Japan.

6.   O.L. Bowie, "Solutions of Plane Crack Problems by Mapping Techniques", Methods of Analysis and Solutions of Crack Problems, G.C. Sih, ed., pp. 1-55, Noordhoff Int. Publ., Leyden, 1973.

7.   H.F. Nied and F. Erdogan, "A Cracked Beam or a Plate Transversely Loaded by a Stamp", Int. J. Solids Structures.

8.   A.C. Kaya and F. Erdogan, "Stress Intensity Factors and COD in an Orthotropic Strip", Int. J. of Fracture, Vol. 16, pp. 171-190, 1980.

9.   B. Gross and J.E. Srawley, "Stress Intensity Factors for Three Point Bend Specimens by Boundary Collocation", NASA-TN D3092, Dec. 1965.

10. J.E. Srawley, "Wide Range Stress Intensity Factor Expressions for ASTM 399 Standard Fracture Toughness Specimens", Int. J. of Fracture, Vol. 12, pp. 475,476, 1976.

11. J.C. Newman, Jr., "An Improved Method of Collocation for the Stress Analysis of Cracked Plates with Various Shaped Boundaries", NASA-TN-D 6376, 1971.

12. N.I. Muskhehshvili, _Some Basic Problems of the Mathematical Theory of Elasticity_, P. Noordhoff Ltd., Groningen-Holland, 1953.

13. F. Erdogan and G.D. Gupta, "On the Numerical Solution of Singular Integral Equations", Quarterly of Applied Mathematics, Vol. 30, pp. 525-534, 1972.

14. G.D. Gupta and F. Erdogan, "The Problem of Edge Cracks in an Infinite Strip", J. Appl. Mech., Vol. 41, Trans. ASME, pp. 1001-1005, 1974.

15. M. Isida, "Analysis of Stress Intensity Factors for Plates Containing Random Array of Cracks", Bulletin of the JSME, Vol. 13, pp. 635-642, 1970.

16. F. Erdogan and G.C. Sih, "On the Crack Extension in Plates under Plane Loading and Transverse Shear", J. Basic Engng., Trans. ASME, Vol. 85, pp. 519-526, 1963.

The functions L_i and R_i which appear in (12):

$$L_1 = -e^{2\alpha H} - 2\alpha H + 1, \quad L_2 = e^{2\alpha H} - 2\alpha H - 1, \quad L_3 = e^{\alpha H} - e^{-\alpha H} ,$$

$$L_4 = e^{-2\alpha H} - 2\alpha H - 1, \quad L_5 = e^{-2\alpha H} + 2\alpha H - 1. \tag{A.1}$$

$$R_i(\alpha) = F_i(\alpha) + G_i(\alpha) + H_i(\alpha) + P_i(\alpha), \quad i = 1,\dots,4 \tag{A.2}$$

$$F_1(a) = - \frac{1}{\kappa+1} \int_a^b f(t) \, \alpha t \, e^{-\alpha t} \, dt ,$$

$$G_1(\alpha) = - \frac{1}{\kappa+1} \cos\alpha B \int_c^d g(t) \alpha t \, e^{-\alpha t} dt ,$$

$$H_1(\alpha) = \frac{1}{\kappa+1} \sin\alpha B \int_c^d h(t) e^{-\alpha t}(\alpha t+1) dt,$$

$$P_1(\alpha) = \frac{e^{-\alpha m} \sin\alpha n \ (\kappa-1-2\alpha m)}{4\mu(\kappa+1)} P ,$$

$$F_2(\alpha) = - \frac{1}{\kappa+1} \int_a^b f(t) \, e^{-\alpha t}(1-\alpha t) dt,$$

$$G_2(\alpha) = - \frac{1}{\kappa+1} \cos\alpha B \int_c^d g(t) e^{-\alpha t}(1-\alpha t) dt,$$

$$H_2(\alpha) = - \frac{1}{\kappa+1} \sin\alpha B \int_c^d h(t) \alpha t \, e^{-\alpha t} \, dt,$$

$$P_2(\alpha) = \frac{e^{-\alpha m}\sin\alpha n(-\kappa-1+2\alpha m)}{4\mu(\kappa+1)} P ,$$

$$F_3(\alpha) = - \frac{1}{\kappa+1} \int_a^b f(t)\alpha(t-H)e^{-\alpha(H-t)} dt,$$

$$G_3(\alpha) = - \frac{1}{\kappa+1} \cos\alpha B \int_c^d g(t)\alpha(t-H)e^{-\alpha(H-t)} dt,$$

$$H_3(\alpha) = \frac{1}{\kappa+1} \sin\alpha B \int_c^d h(t)e^{-\alpha(H-t)}[\alpha(H-t)+1] dt,$$

$$P_3(\alpha) = \frac{e^{-\alpha(H-m)} \sin\alpha n[\kappa-1-2\alpha(H-m)]}{4\mu(\kappa+1)} P ,$$

$$F_4(\alpha) = - \frac{1}{\kappa+1} \int_a^b f(t)e^{-\alpha(H-t)} [1-\alpha(H-t)]dt ,$$

$$G_4(\alpha) = - \frac{1}{\kappa+1} \cos\alpha B \int_c^d g(t)e^{-\alpha(H-t)} [1-\alpha(H-t)] dt,$$

$$H_4(\alpha) = - \frac{1}{\kappa+1} \sin\alpha B \int_c^d h(t)\alpha(t-H)e^{-\alpha(H-t)}dt,$$

$$P_4(\alpha) = \frac{e^{-\alpha(H-m)} \sin\alpha n [\kappa+1-2\alpha(H-m)]}{4\mu(\kappa+1)} P .$$
(A.3)

The kernels $k_{ij}(x,t)$ and the functions $k_{i4}(x)$, $(i,j=1,2,3)$:

$k_{11}(x,t) = G(x,t) + G(x-H,t-H) + k_{f1}(x,t)$,

$k_{12}(x,t) = 2[Q_1(B,x,t) + Q_2(B,x,t) - Q_2(B,H-x,H-t) + k_{g1}(x,t)]$

$k_{13}(x,t) = 2[Q_3(B,x,t) + Q_4(B,x,t) + Q_4(B,H-x,H-t) + k_{h1}(x,t)]$,

$k_{21}(x,t) = Q_1(B,x,t) + Q_2(B,x,t) - Q_2(B,H-x,H-t) + k_{f2}(x,t)$,

$k_{22}(x,t) = G(x,t) + G(x-H,t-H) + Q_1(2B,x,t) + Q_2(2B,x,t)$

$\qquad - Q_2(2B,H-x,H-t) + k_{g2}(x,t)$,

$k_{23}(x,t) = Q_3(2B,x,t) + Q_4(2B,x,t) + Q_4(2B,x,t) + k_{h2}(x,t)$,

$k_{31}(x,t) = Q_5(B,x,t) + Q_6(B,x,t) + Q_6(B,H-x,H-t) + k_{f3}(x,t)$,

$k_{32}(x,t) = Q_5(2B,x,t) + Q_6(2B,x,t) + Q_6(2B,H-x,H-t) + k_{g3}(x,t)$,

$k_{33}(x,t) = G(x,t) + G(x-H,t-H) + Q_7(B,x,t) + Q_8(B,x,t)$

$\qquad - Q_8(B,H-x,H-t) + k_{h3}(x,t)$, $\hfill$ (B.1)

where,

$$G(x,t) = - \frac{1}{t+x} + \frac{6x}{(t+x)^2} - \frac{4x^2}{(t+x)^3} \quad , \qquad (B.2)$$

$$Q_1(B,x,t) = \frac{(t-x)[(t-x)^2 + 3B^2]}{[B^2 + (t-x)^2]^2} \quad ,$$

$$Q_2(B,x,t) = \frac{2(t+x)}{B^2 + (t+x)^2} - \frac{(3t+x)[(t+x)^2-B^2]}{[B^2 + (t+x)^2]^2} + \frac{4xt(t+x)[(t+x)^2-3B^2]}{[B^2 + (t+x)^2]^3} \quad ,$$

$$Q_3(B,x,t) = \frac{B[(t-x)^2-B^2]}{[B^2 + (t-x)^2]^2} \quad ,$$

$$Q_4(B,x,t) = \frac{B}{B^2+(t+x)^2} + \frac{2B(3t-x)(t+x)}{[B^2+(t+x)^2]^2} - \frac{4Bxt[3(t+x)^2-B^2]}{[B^2+(t+x)^2]^3} \ ,$$

$$Q_5(B,x,t) = \frac{B[B^2-(t-x)^2]}{[B^2+(t-x)^2]^2} \ ,$$

$$Q_6(B,x,t) = - \frac{B}{B^2+(t+x)^2} + \frac{2B(t+x)^2}{[B^2+(t+x)^2]^2} - \frac{4Bxt[3(t+x)^2-B^2]}{[B^2+(t+x)^2]^3}$$

$$Q_7(B,x,t) = \frac{(x-t)[(t-x)^2-4B^2]}{[4B^2+(t-x)^2]^2} \ ,$$

$$Q_8(B,x,t) = \frac{(t-x)[(t+x)^2-4B^2]}{[4B^2+(t+x)^2]^2} - \frac{4xt(t+x)[(t+x)^2-12B^2]}{[4B^2+(t+x)^2]^3} \ , \tag{B.3}$$

$$k_{f1}(x,t) = \int_0^\infty \frac{1}{D(\alpha)} [R_1(x,t,\alpha)+R_2(x,t,\alpha)-R_1(H-x,H-t,\alpha)-R_2(H-x,H-t,\alpha)]d\alpha,$$

$$k_{g1}(x,t) = \int_0^\infty \frac{1}{D(\alpha)} [R_1(x,t,\alpha)+R_2(x,t,\alpha)-R_1(H-x,H-t,\alpha)-R_2(H-x,H-t,\alpha)]\cos(\alpha B)d\alpha,$$

$$k_{h1}(x,t) = \int_0^\infty \frac{1}{D(\alpha)} [S_1(x,t,\alpha)+S_2(x,t,\alpha)+S_1(H-x,H-t,\alpha)+S_2(H-x,H-t,\alpha)]\sin(\alpha B)d\alpha,$$

$$k_{f2}(x,t) = \int_0^\infty \frac{1}{D(\alpha)} [R_1(x,t,\alpha)+R_2(x,t,\alpha)-R_1(H-x,H-t,\alpha)-R_2(H-x,H-t,\alpha)]\cos(\alpha B)d\alpha,$$

$$k_{g2}(x,t) = 2 \int_0^\infty \frac{1}{D(\alpha)} [R_1(x,t,\alpha)+R_2(x,t,\alpha)-R_1(H-x,H-t,\alpha)-R_2(H-x,H-t,\alpha)]\cos^2(\alpha B)d\alpha,$$

$$k_{h2}(x,t) = \int_0^\infty \frac{1}{D(\alpha)} [S_1(x,t,\alpha)+S_2(x,t,\alpha)-S_1(H-x,H-t,\alpha)-S_2(H-x,H-t,\alpha)]\sin(2\alpha B)d\alpha,$$

$$k_{f3}(x,t) = \int_0^\infty \frac{1}{D(\alpha)} [T_1(x,t,\alpha)+T_2(x,t,\alpha)+T_1(H-x,H-t,\alpha)+T_2(H-x,H-t,\alpha)]\sin(\alpha B)d\alpha,$$

$$k_{g3}(x,t) = \int_0^\infty \frac{1}{D(\alpha)} [T_1(x,t,\alpha)+T_2(x,t,\alpha)+T_1(H-x,H-t,\alpha)+T_2(H-x,H-t,\alpha)]\sin(2\alpha B)d\alpha,$$

$$k_{h3}(x,t) = 2 \int_0^\infty \frac{1}{D(\alpha)} [U_1(x,t,\alpha)+U_2(x,t,\alpha)-U_1(H-x,H-t,\alpha)-U_2(H-x,H-t,\alpha)]\sin^2(\alpha B)d\alpha,$$

$$\tag{B.4}$$

$$R_1(x,t,\alpha) = [4\alpha^2H^2-e^{-2\alpha H})(2-3\alpha t-\alpha x+2\alpha^2 xt) + 2-3\alpha t-\alpha x+2\alpha^2 xt$$
$$-2\alpha^2H^2 + 2\alpha^2 tH + 2\alpha^2 xH - 4\alpha H]e^{-\alpha(t+x)} \ ,$$

-23-

$$R_2(x,t,\alpha) = [(1-e^{-2\alpha H})(\alpha x-\alpha t-2)-2\alpha H(\alpha x-2+2\alpha^2 xt-2\alpha^2 xH-3\alpha t+3\alpha H)]e^{\alpha(t-x)},$$

$$(B.5)$$

$$S_1(x,t,\alpha) = [(4\alpha^2 H^2-e^{-2\alpha H})(1-\alpha x+3\alpha t-2\alpha^2 xt)+1-\alpha x+3\alpha t-2\alpha^2 xt+2\alpha^2 H^2$$
$$-2\alpha^2 xH + 2\alpha H - 2\alpha^2 tH]e^{-\alpha(t+x)} ,$$

$$S_2(x,t,\alpha) = [(1-e^{-2\alpha H})(\alpha x-1-\alpha t)+2\alpha H(\alpha x-1+2\alpha^2 xH-2\alpha^2 xt-3\alpha H+3\alpha t)]e^{\alpha(t-x)} ,$$

$$(B.6)$$

$$T_1(x,t,\alpha) = [(4\alpha^2 H^2-e^{-2\alpha H})(-1+\alpha x+\alpha t-2\alpha^2 xt)+2\alpha^2 H^2-2\alpha^2 xt-1+\alpha x+\alpha t$$
$$+2\alpha H-2\alpha^2 xH-2\alpha^2 tH]e^{-\alpha(t+x)},$$

$$T_2(x,t,\alpha) = [(1-e^{-2\alpha H})(\alpha t+1-\alpha x)+2\alpha H(\alpha x-1+2\alpha^2 xt-2\alpha^2 xH-\alpha t+\alpha H)]e^{\alpha(t-x)},$$

$$(B.7)$$

$$U_1(x,t,\alpha) = [(4\alpha^2 H^2-e^{-2\alpha H})(\alpha x+2\alpha^2 xt-\alpha t)+\alpha x+2\alpha^2 xt-\alpha t-2\alpha^2 H^2+2\alpha^2 xH$$
$$+ 2\alpha^2 tH]e^{-\alpha(t+x)} ,$$

$$U_2(x,t,\alpha) = [(1-e^{-2\alpha H})(\alpha t-\alpha x)-2\alpha H(\alpha x+2\alpha^2 xH-2\alpha^2 xt-\alpha H+\alpha t)]e^{\alpha(t-x)} ,$$

$$(B.8)$$

$$k_{14}(x) = - \frac{2}{\pi(\kappa+1)} [V_1(x,0) + V_2(m,x,0) + V_2(H-m,H-x,0)],$$

$$k_{24}(x) = - \frac{1}{\pi(\kappa+1)} [V_1(x,B)+V_1(x,-B)+V_2(m,x,B)+V_2(m,x,-B)$$
$$+ V_2(H-m,H-x,B) + V_2(H-m,H-x,-B) + k_{p1}(x)] ,$$

$$k_{34}(x) = - \frac{1}{\pi(\kappa+1)} [Y_1(x,B)-Y_1(x,-B)+Y_2(m,x,B)-Y_2(m,x,-B)$$
$$-Y_2(H-m,H-x,B)+Y_2(H-m,H-x,-B)+k_{p2}(x)] \qquad (B.9)$$

$$V_1(x,B) = - \frac{(\kappa+3)(B-n)}{2[(x-m)^2 + (B-n)^2]} + \frac{2(x-m)^2(B-n)}{[(x-m)^2 + (B-n)^2]^2} ,$$

$$V_2(m,x,B) = - \frac{(1+3\kappa)(B-n)}{2[(x+m)^2 + (B-n)^2]} + \frac{2(\kappa x+3m)(B-n)(x+m)}{[(x+m)^2 + (B-n)^2]^2}$$

$$- \frac{4mx(B-n)[3(x+m)^2-(B-n)^2]}{[(x+m)^2 + (B-n)^2]^3} , \qquad \text{(B.10)}$$

$$Y_1(x,B) = - \frac{(\kappa+3)(x-m)}{2[(x-m)^2+(B-n)^2]} + \frac{2(x-m)^3}{[(x-m)^2+(B-n)^2]^2} ,$$

$$Y_2(m,x,B) = - \frac{(\kappa+1)(x+m)}{2[(x+m)^2+(B-n)^2]} + \frac{(\kappa x+m)[(x+m)^2-(B-n)^2]}{[(x+m)^2+(B-n)^2]^2}$$

$$- \frac{4mx(x+m)[(x+m)^2-3(B-n)^2]}{[(x+m)^2+(B-n)^2]^3} , \qquad \text{(B.11)}$$

$$k_{p1}(x) = \int_0^\infty [X_1(m,x,\alpha) + X_2(m,x,\alpha) + X_1(H-m,H-x,\alpha)$$

$$+ X_2(H-m,H-x,\alpha)]\sin(\alpha n)\sin(\alpha B)d\alpha,$$

$$k_{p2}(x) = \int_0^\infty [Z_1(m,x,\alpha)+Z_2(m,x,\alpha)-Z_1(H-m,H-x,\alpha)$$

$$-Z_2(H-m,H-x,\alpha)]\sin(\alpha n)\sin(\alpha B)d\alpha, \qquad \text{(B.12)}$$

$$X_1(m,x,\alpha) = \{[\kappa-2\alpha m)(2\alpha x-3)-1](e^{-2\alpha H}-4\alpha^2 H^2-1)$$

$$+ 2\alpha H(2\alpha m-2\alpha H+2\alpha x-3-\kappa)\}e^{-\alpha(m+x)} ,$$

$$X_2(m,x,\alpha) = \{ (1-e^{-2\alpha H})(2\alpha m-2\alpha x+\kappa+3)$$

$$2\alpha H[2\alpha x(\kappa+2\alpha m-2\alpha H)-3\kappa+6\alpha H-6\alpha m-1]\}e^{\alpha(m-x)}$$

$$\text{(B.13)}$$

$$Z_1(m,x,\alpha) = \{ (1-e^{-2\alpha H}+4\alpha^2 H^2)[(\kappa-2\alpha m)(2\alpha x-1)-1]$$

$$+ 2\alpha H(2\alpha H-2\alpha m-2\alpha x+2+\kappa)\}e^{-\alpha(m+x)} ,$$

$$Z_2(m,x,\alpha) = \{ (1-e^{-2\alpha H})(2\alpha x-2\alpha m-\kappa-1) - 2\alpha H[2\alpha x(\kappa+2\alpha m-2\alpha H)$$

$$- \kappa - 1 + 2\alpha H - 2\alpha m]\}e^{\alpha(m-x)} . \qquad \text{(B.14)}$$
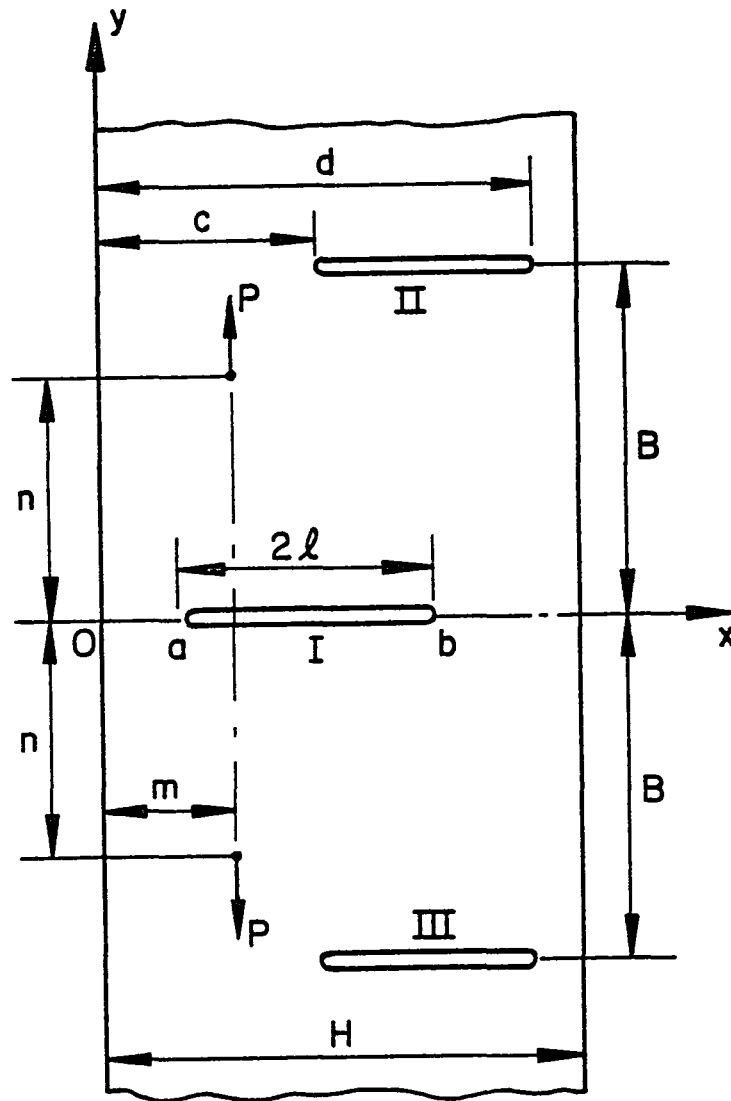
Figure 1.   The basic crack geometry.
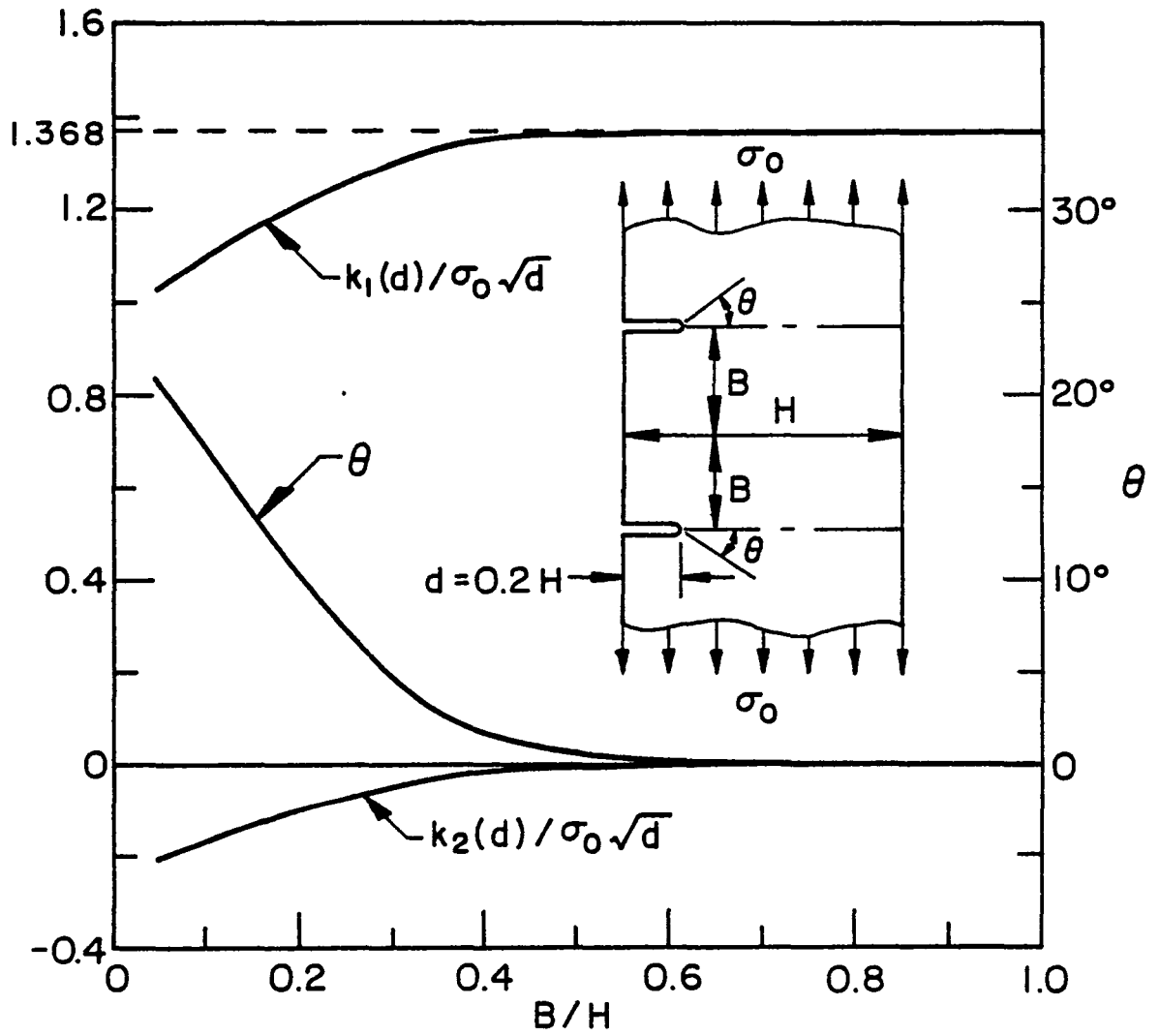
Figure 2.   Stress intensity factors and probable crack propagation
angle in an infinite strip containing two edge cracks under
uniform tension, d=0.2H.
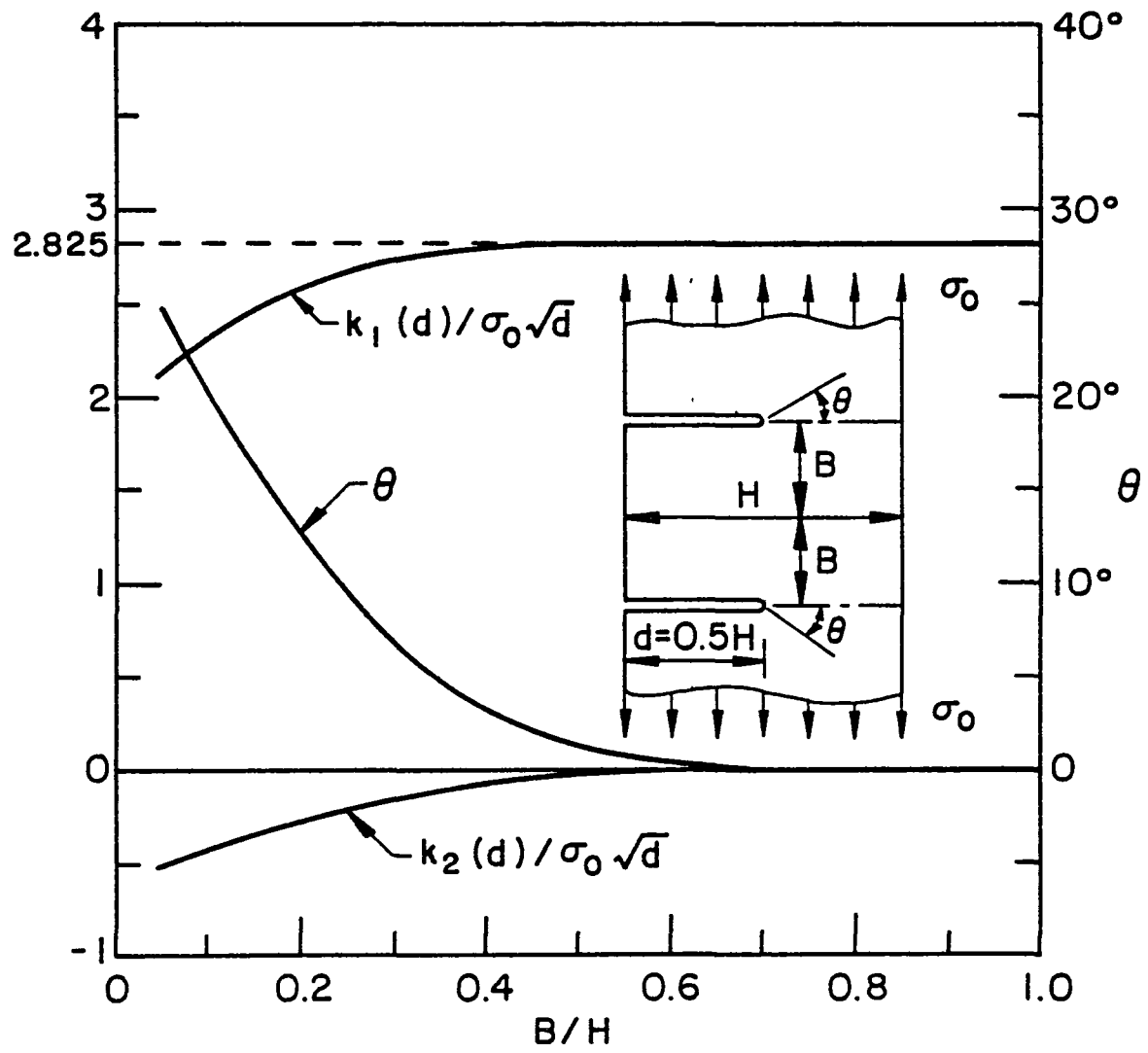
Figure 3.   Same as Figure 2, d=0.5H.
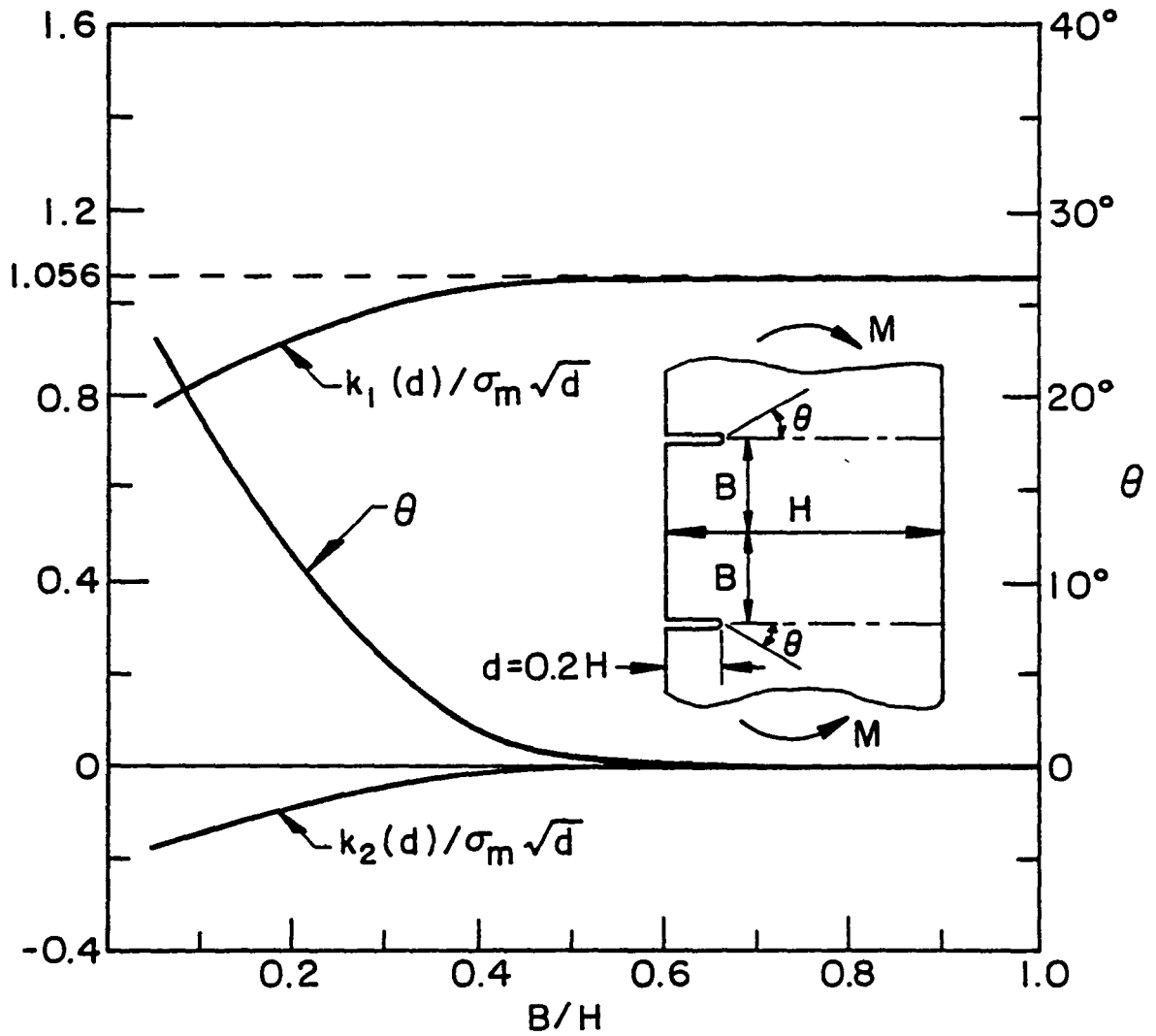
Figure 4.   Stress intensity factors and probable crack propagation angle in an infinite strip with two edge cracks under bending, d=0.2H.
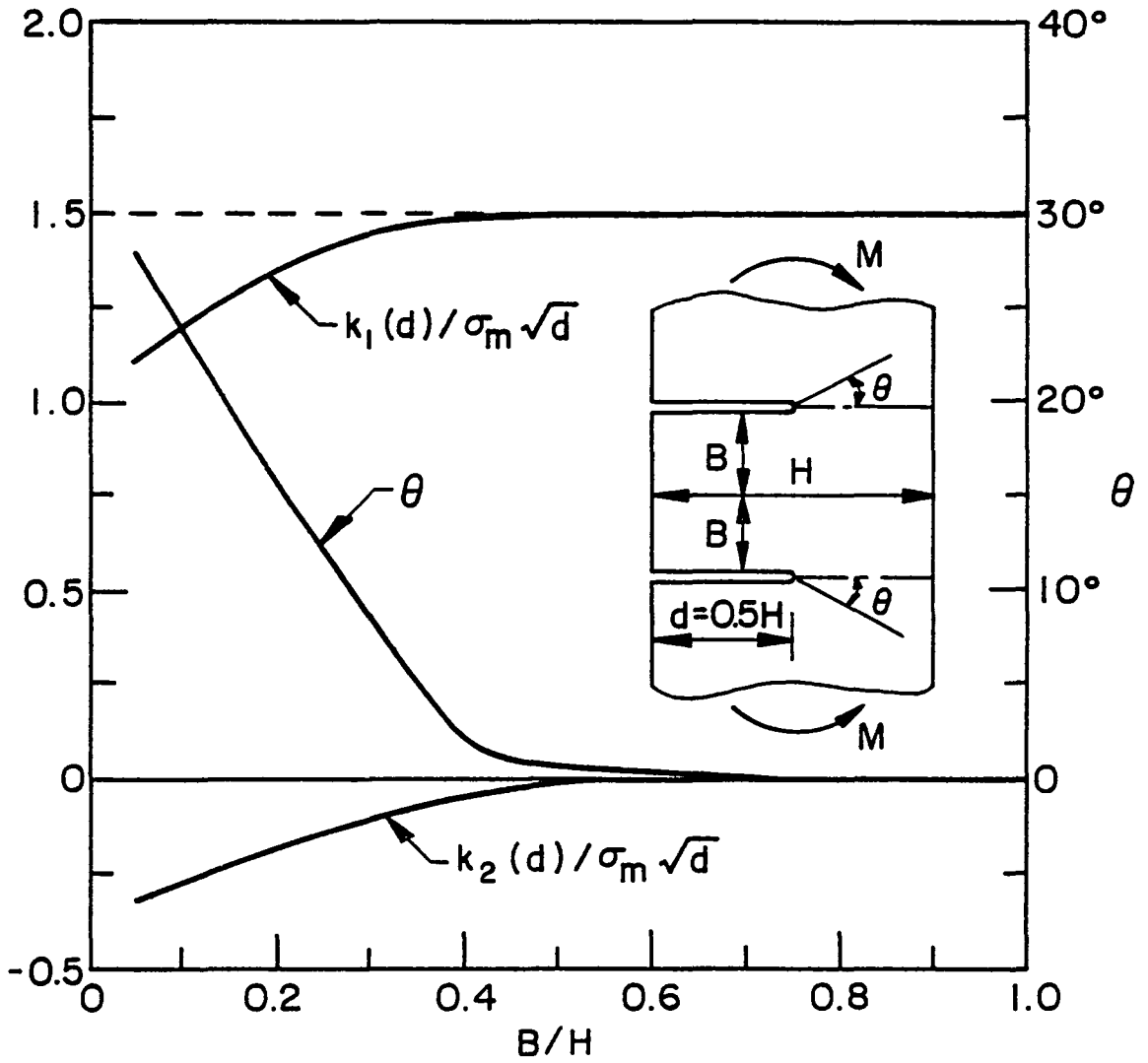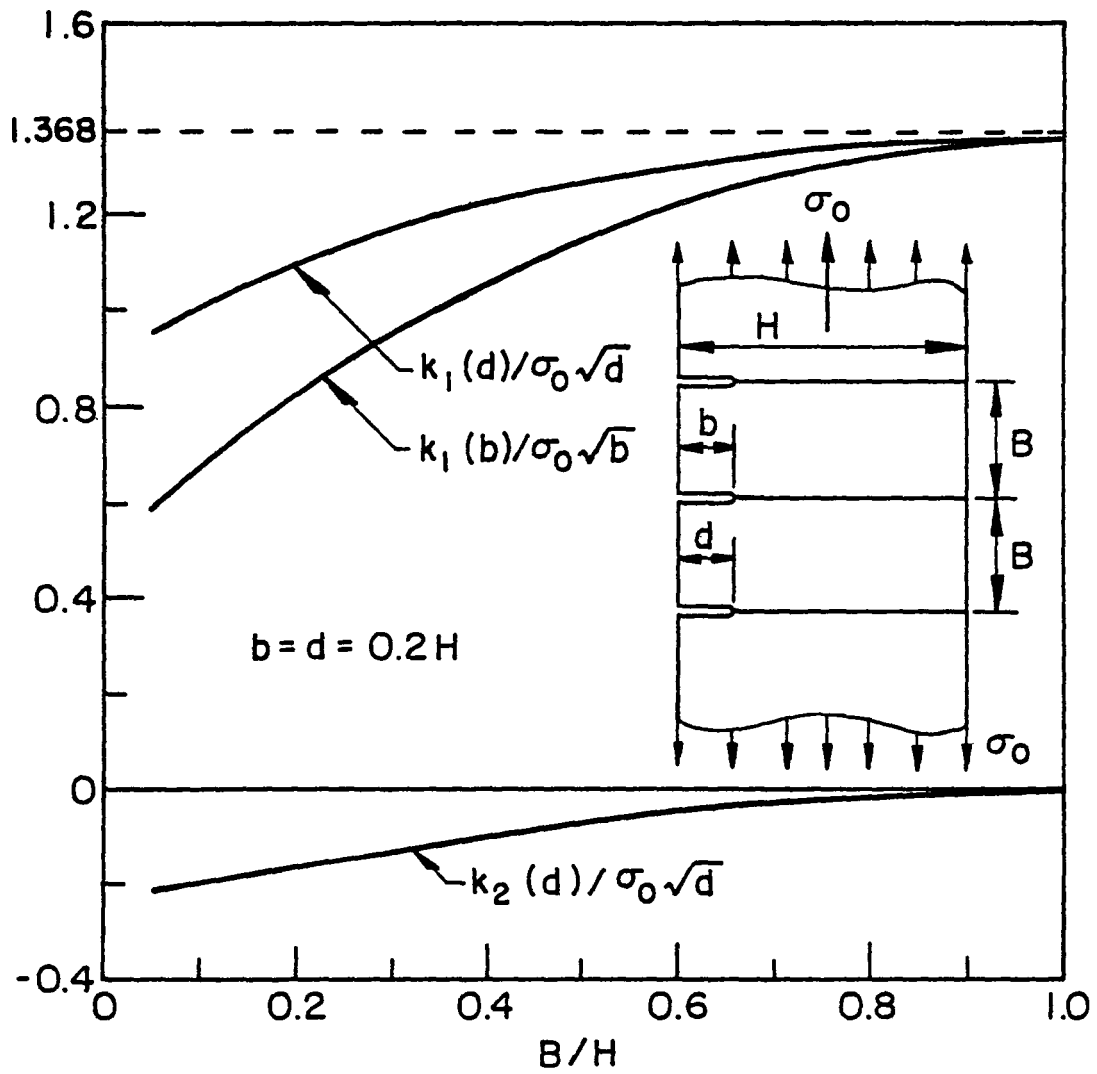
Figure 5.   Same as Figure 4, d=0.5H.

Figure 6. Stress intensity factors in an infinite strip containing three edge cracks under uniform tension, d=b=0.2H.
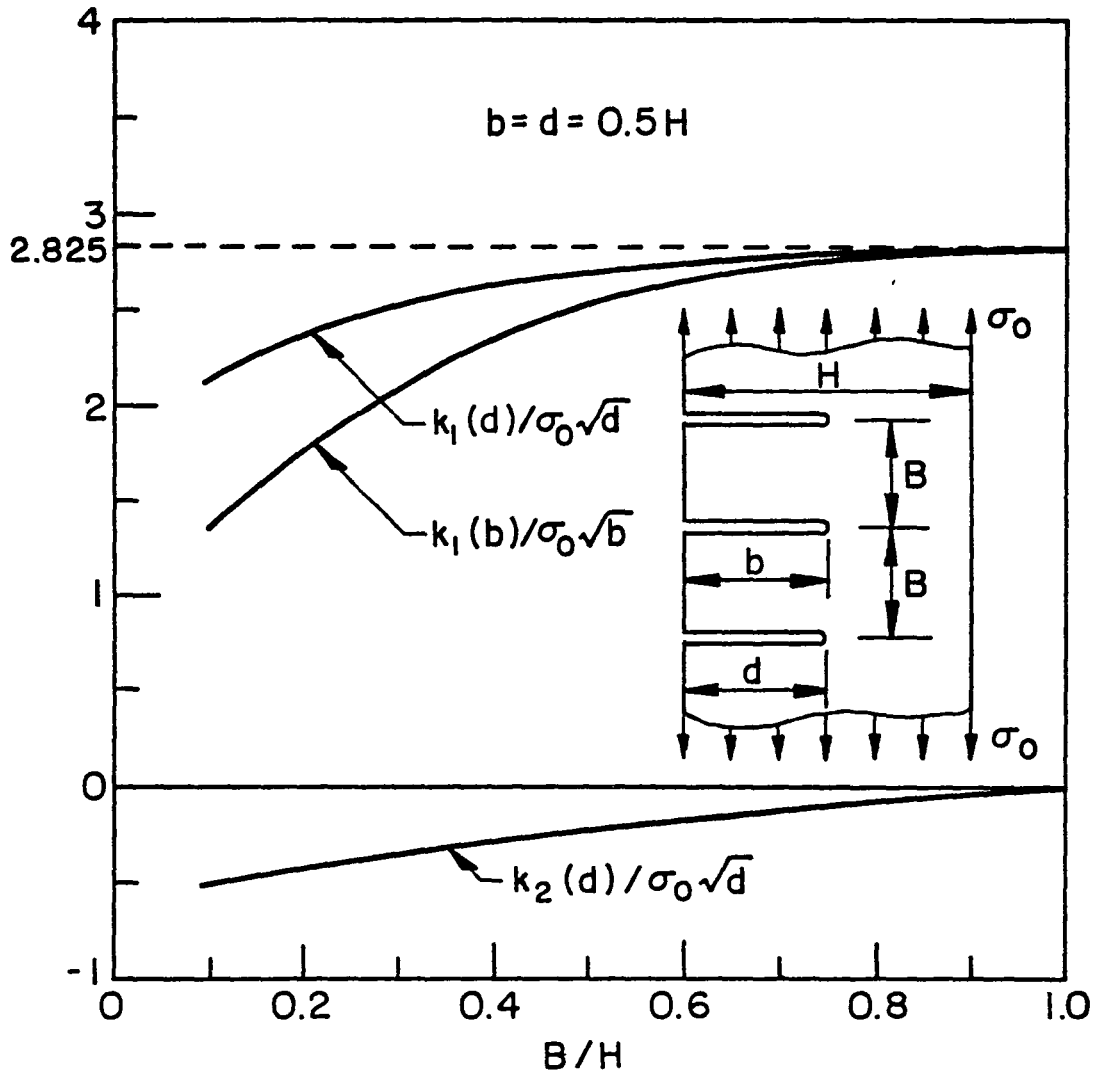
Figure 7. Same as Figure 6, d=b=0.5H.
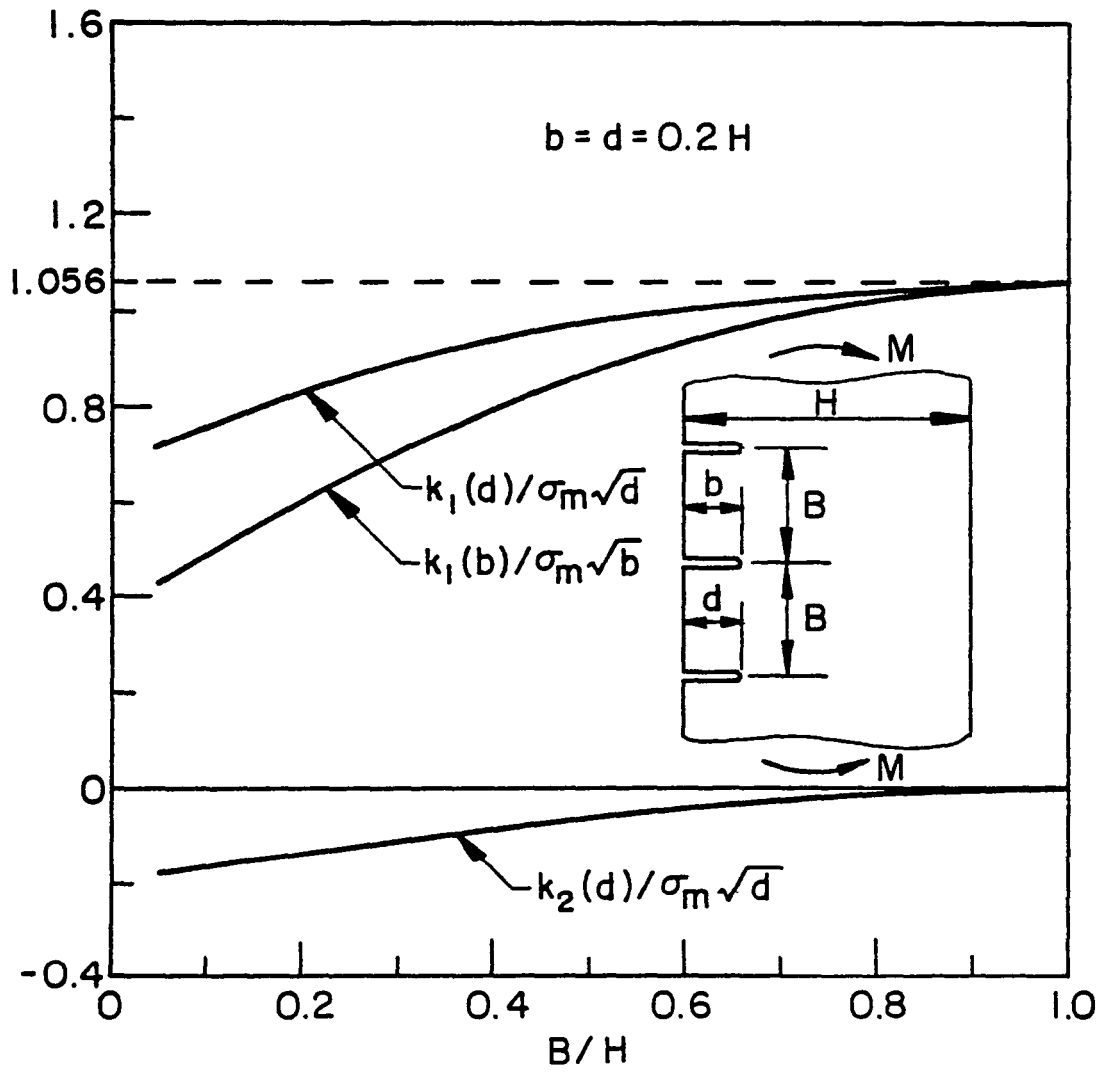
Figure 8.   Stress intensity factors in an infinite strip containing three edge cracks under bending, $d=b=0.2H$, $\sigma_m=6M/H^2$.
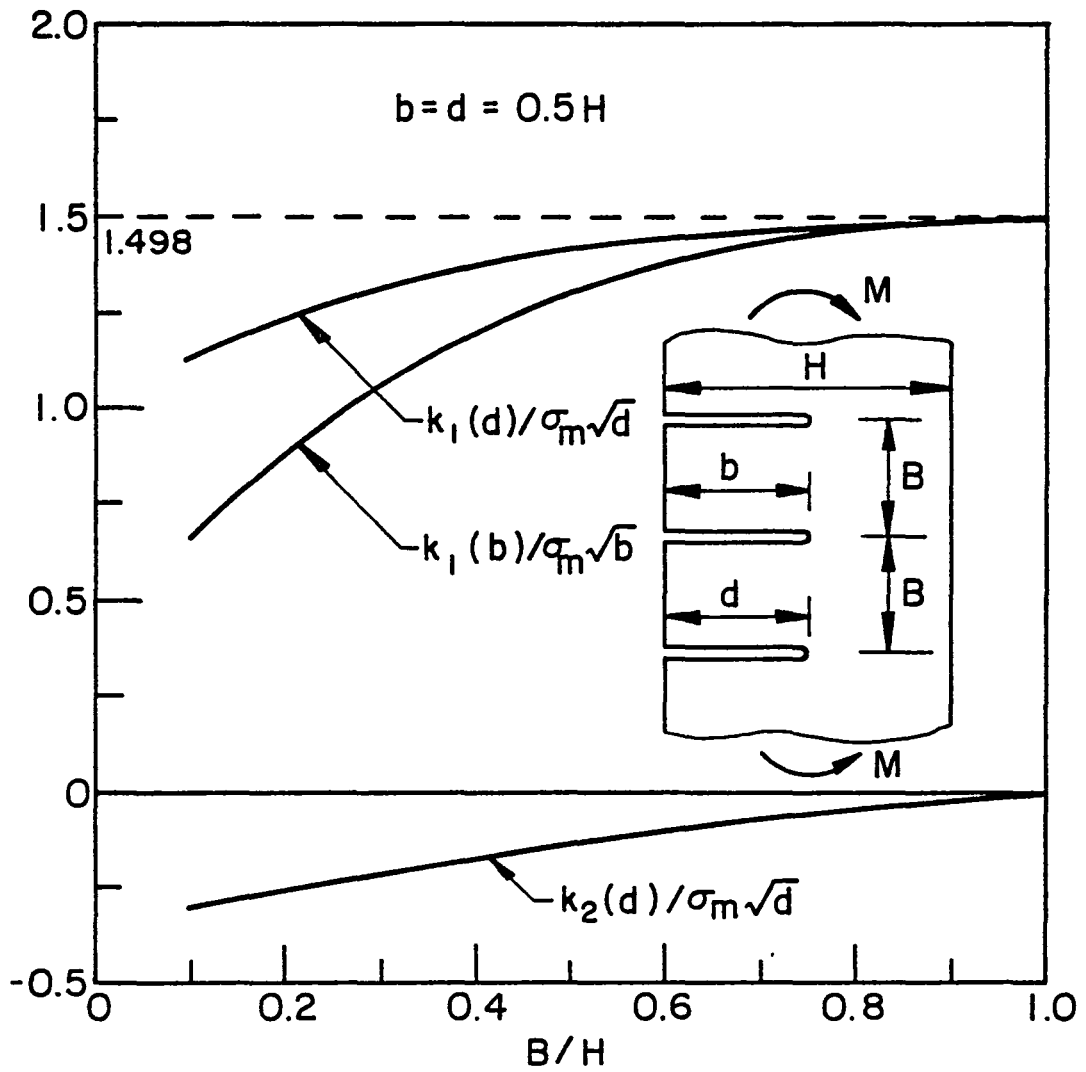
Figure 9.   Same as Figure 8, d=b=0.5H, σ_m=6M/H^2.
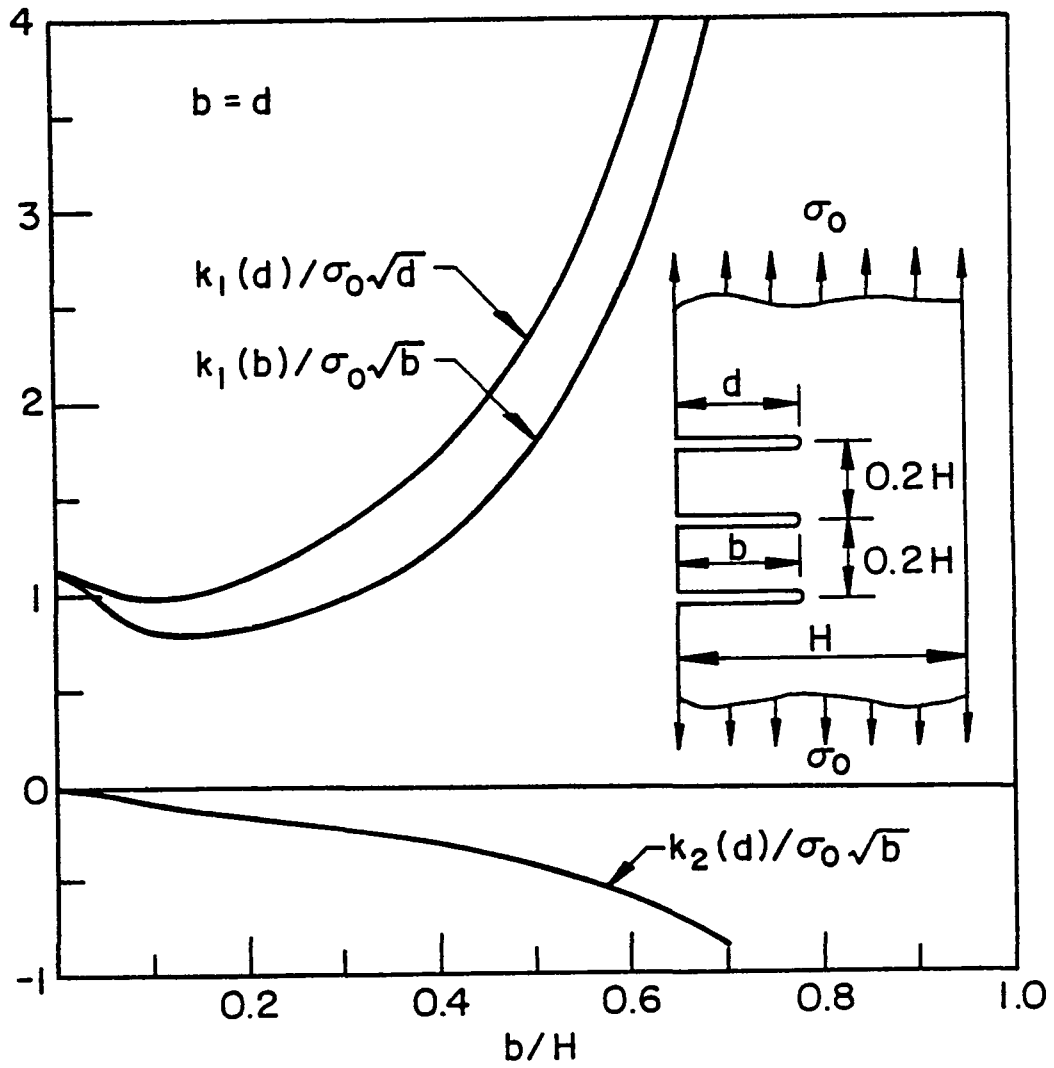
Figure 10.   The effect of the crack depth on the stress intensity factors in an infinite strip under tension, B=0.2H.
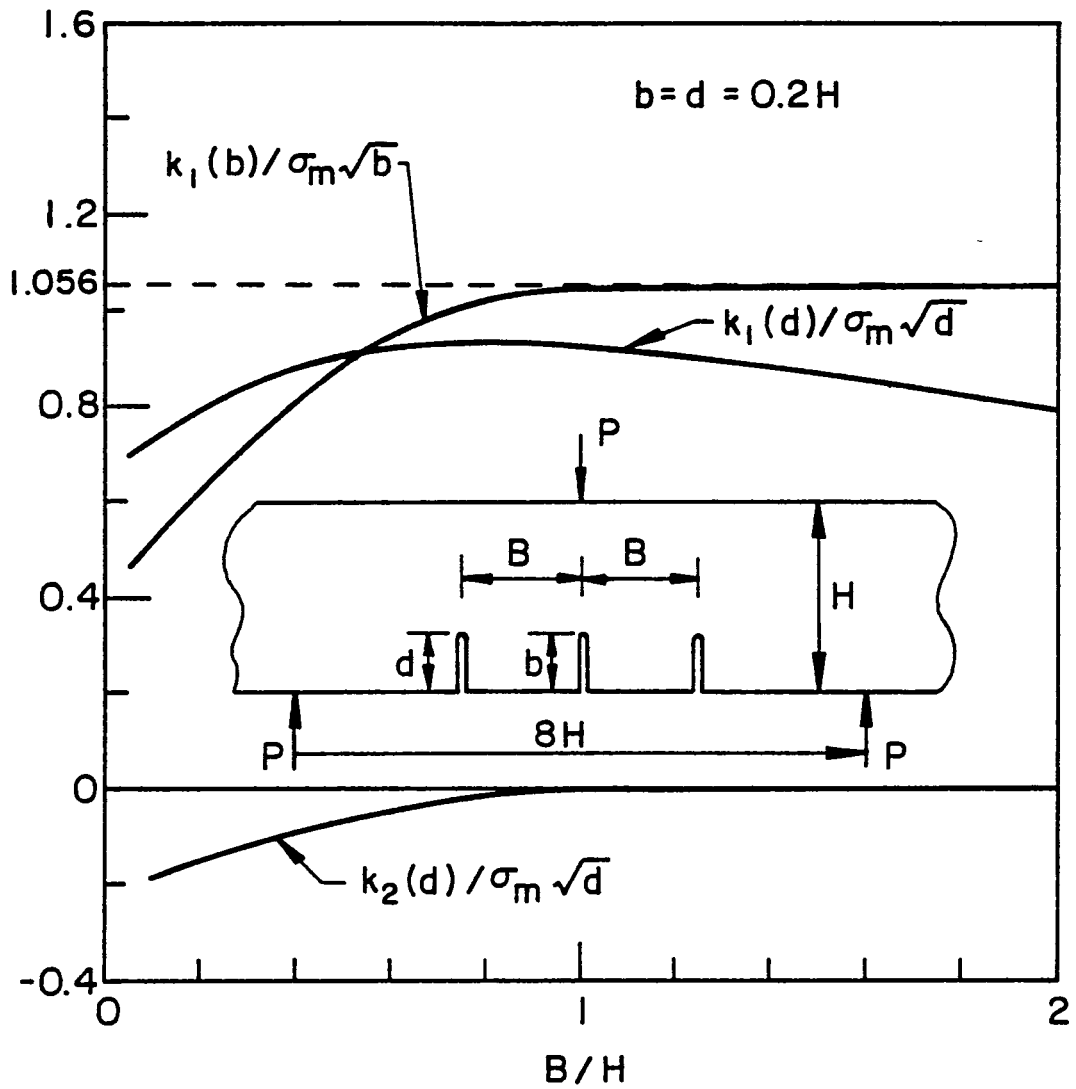
Figure 11.   Stress intensity factors in an infinite strip containing
              edge cracks and subjected to three point bending, σ_m =
              $6M/H^2$ = $24P/H$.
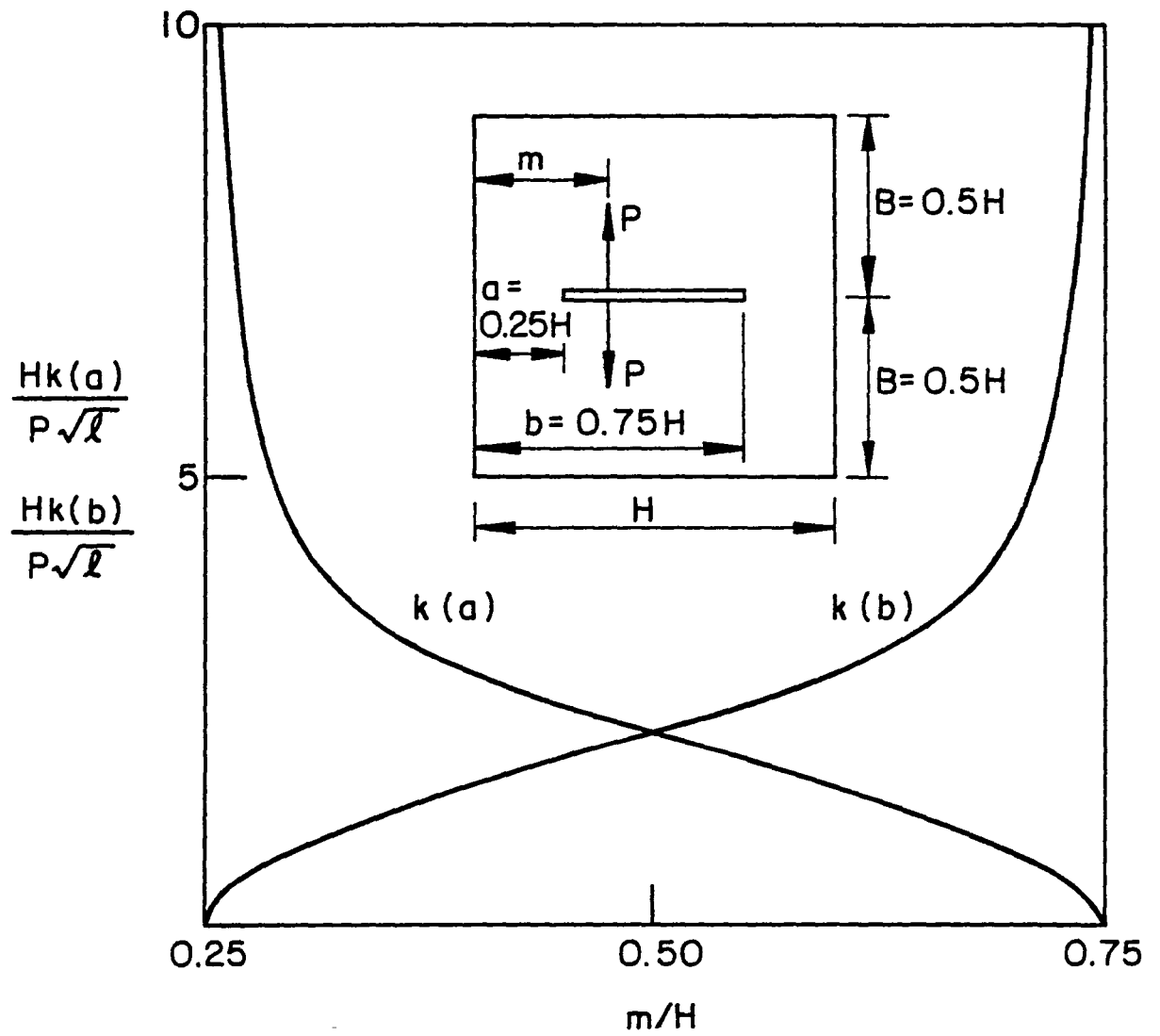
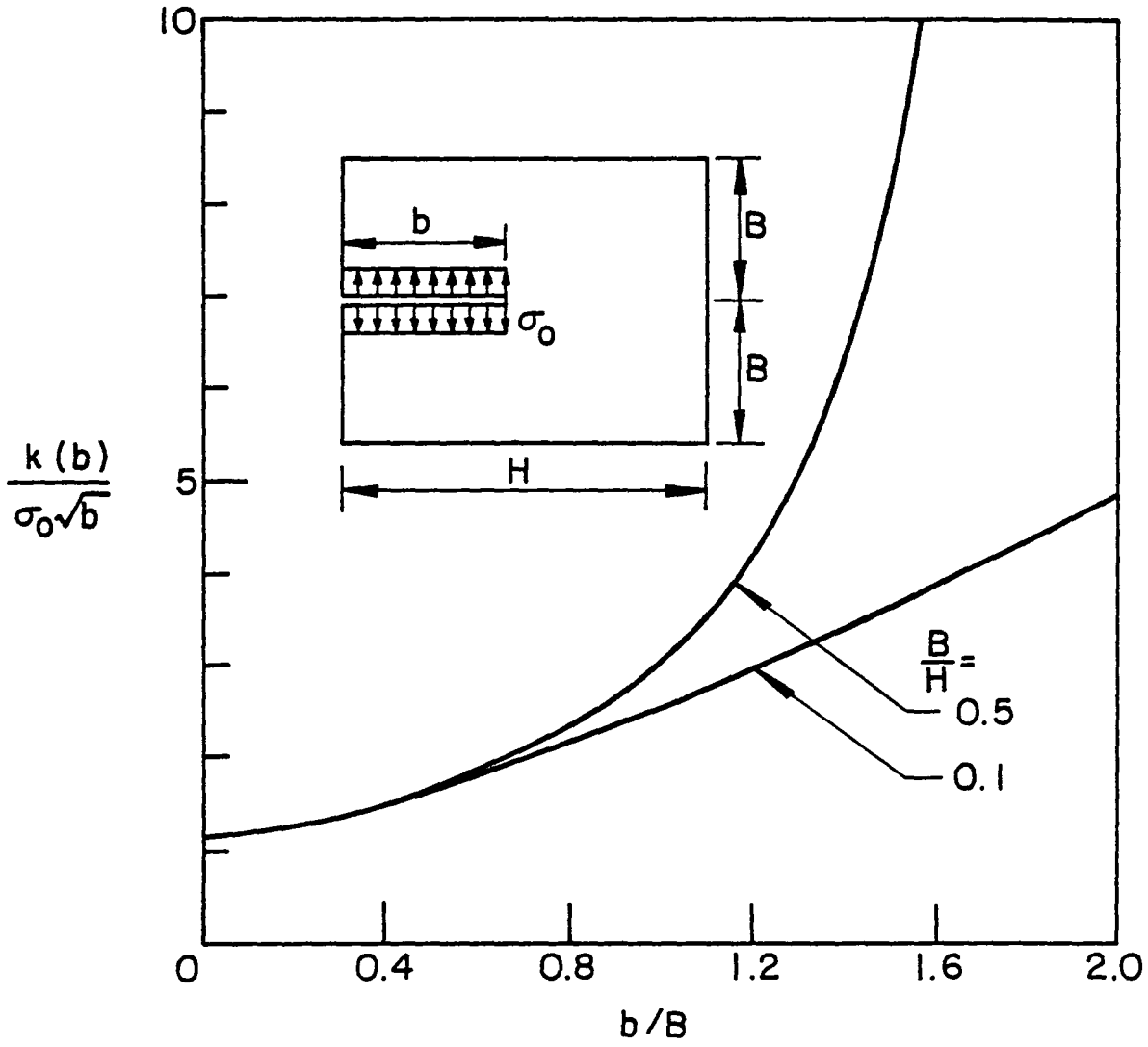Figure 12.   Stress intensity factor in a square plate containing a wedge-loaded central crack.

Figure 13.   Stress intensity factor in a uniformly loaded rectangular plate naving an edge crack.
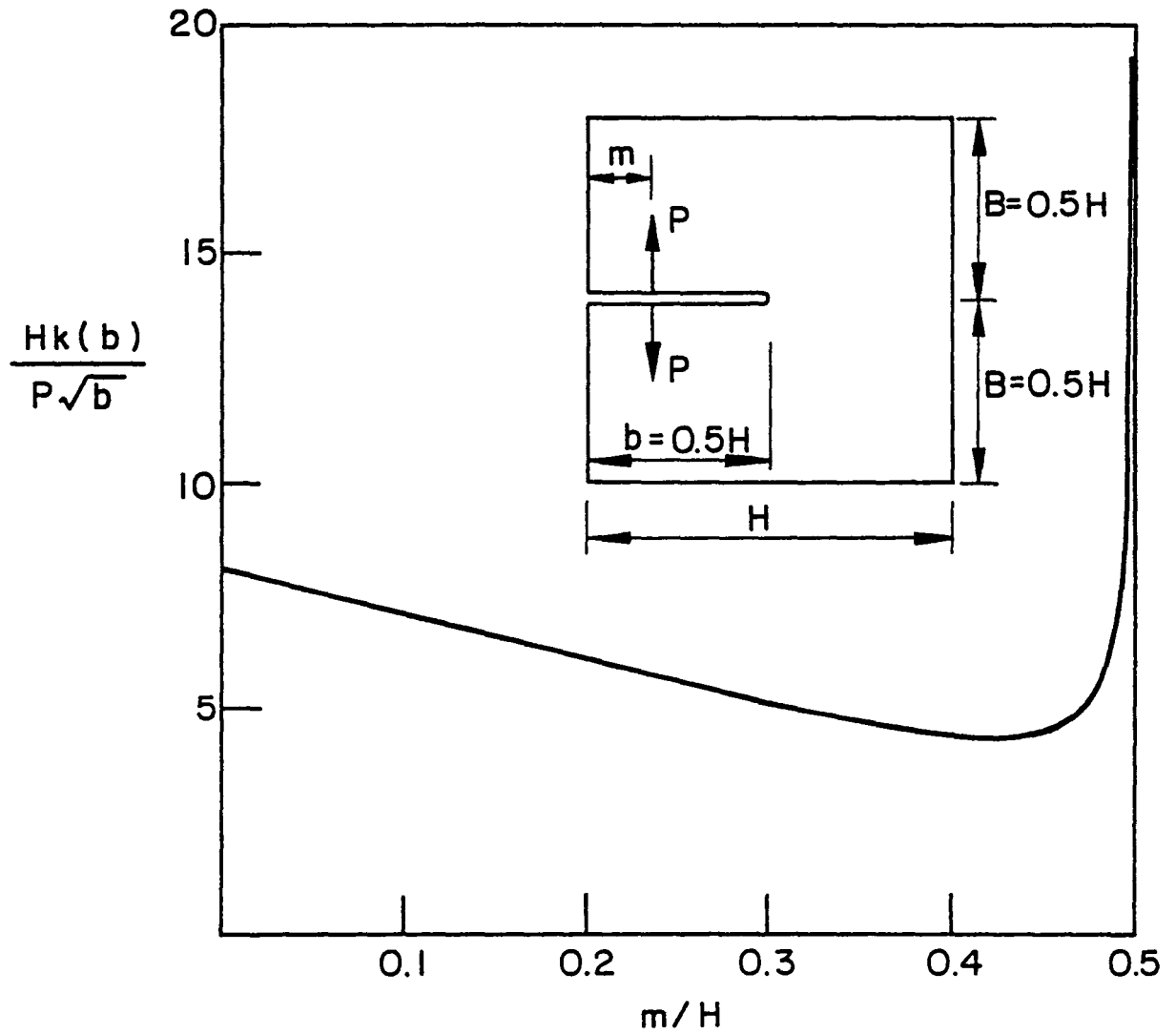
Figure 14.   Stress intensity factor in a square plate with an edge
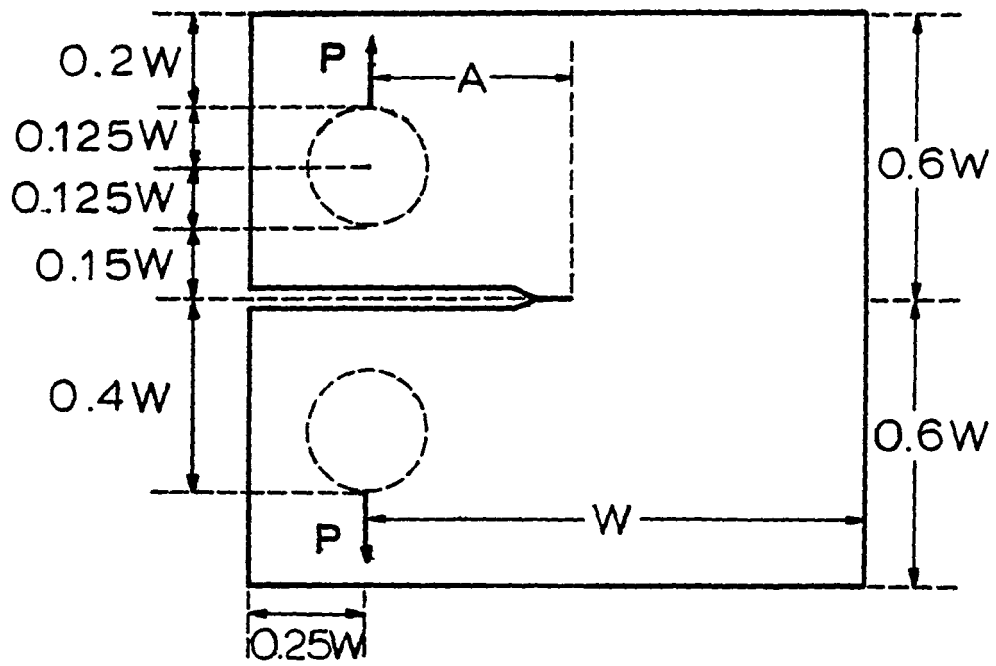crack under wedge loading.

Figure 15.   Notation for the compact tension specimen.

End of Document